A Thesis

entitled

Monte Carlo Investigation on the Effect of Heterogeneities on Strut Adjusted Volume Implant (SAVI) Dosimetry

by

Craig Koontz

Submitted to the Graduate Faculty as partial fulfillment of the requirements for the Master of Science in Biological Sciences Degree in Medical Physics

____

Dr. David Pearson, Committee Chair

____

Dr. E. Ishmael Parsai, Committee Member

____

Dr. Michael Dennis, Committee Member

____

Dr. Patricia Komuniecki, Dean
College of Graduate Studies

The University of Toledo
August 2013

An Abstract of

Monte Carlo Investigation on the Effect of Heterogeneities on Strut Adjusted Volume Implant (SAVI) Dosimetry

by

Craig Koontz

Submitted to the Graduate Faculty as partial fulfillment of the requirements for the Master of Science in Biological Sciences Degree in Medical Physics

The University of Toledo
August 2013

Breast cancer is the most prevalent cancer for women with more than 225,000 new cases diagnosed in the United States in 2012 (ACS, 2012). With the high prevalence, comes an increased emphasis on researching new techniques to treat this disease. Accelerated partial breast irradiation (APBI) has been used as an alternative to whole breast irradiation (WBI) in order to treat occult disease after lumpectomy. Similar recurrence rates have been found using ABPI after lumpectomy as with mastectomy alone, but with the added benefit of improved cosmetic and psychological results. Intracavitary brachytherapy devices have been used to deliver the APBI prescription. However, inability to produce asymmetric dose distributions in order to avoid overdosing skin and chest wall has been an issue with these devices. Multi-lumen devices were introduced to overcome this problem. Of these, the Strut-Adjusted Volume Implant (SAVI) has demonstrated the greatest ability to produce an asymmetric dose distribution, which would have greater ability to avoid skin and chest wall dose, and thus allow more women to receive this type of treatment. However, SAVI treatments come with inherent heterogeneities including variable backscatter due to the proximity to the tissue-air and

tissue-lung interfaces and variable contents within the cavity created by the SAVI. The dose calculation protocol based on TG-43 does not account for heterogeneities and thus will not produce accurate dosimetry; however Acuros, a model-based dose calculation algorithm manufactured by Varian Medical Systems, claims to accurately account for heterogeneities. Monte Carlo simulation can calculate the dosimetry with high accuracy. In this thesis, a model of the SAVI will be created for Monte Carlo, specifically using MCNP code, in order to explore the affects of heterogeneities on the dose distribution. This data will be compared to TG-43 and Acuros calculated dosimetry to explore their accuracy.

For Janelle.

Acknowledgments

I would like to express my appreciation to all of those who have helped me to complete this project. Specifically, I would like to thank Dr. Pearson for his guidance and Dr. Parsai for his leadership and support. Assistance from Nick Sperling and Sean Tanny throughout the year has been invaluable. Dr. Shvydka's instruction was always enlightening and put a smile on my face. My thanks are extended to Dr. Dennis for teaching me everything I know about diagnostic physics, and sailing. I would also like to thank Drs. Feldmeier and Chen for their patience, teaching, and stories throughout the year. Finally, I would like to thank all my student colleagues. David, David, Jason, Justin, and Nicki: these past two years would have been much more difficult without your support, discourse, and humor.

Contents

Contents

List of Tables

List of Figures

List of Abbreviations

3D…………………...Three Dimensional

AAPM……………… American Association of Physicists in Medicine
APBI……………….. Accelerated Partial Breast Irradiation

BCT ………………...Breast Conserving Therapy
BV…………………..BrachyVision

CT………………….. Computed Tomography
CW………………….Chest Wall

D90………………… Minimum dose covering 90% of the volume
DMF……………….. Dose Modification Factor

EPID……………….. Electronic Portal Imaging Device

HDR………………...High Dose Rate

IMRT………………. Intensity Modulated Radiation Therapy

LDR………………... Lose Dose Rate

MBDCA…………….Model Based Dose Calculation Methods
MC………………….Monte Carlo
MCNP……………… Monte Carlo Neutral Particle

PBI………………….Partial Breast Irradiation
PTV…………………Planning Treatment Volume

RTOG……………….Radiation Therapy Oncology Group

SAVI……………….. Strut Adjusted Volume Implant

TG-43……………….AAPM Task Group No. 43 Updated Report
TG-186……………...AAPM Task Group No. 186 Report
TPS………………….Treatment Planning System

WBI…………………Whole Breast Irradiation

Chapter 1

Introduction

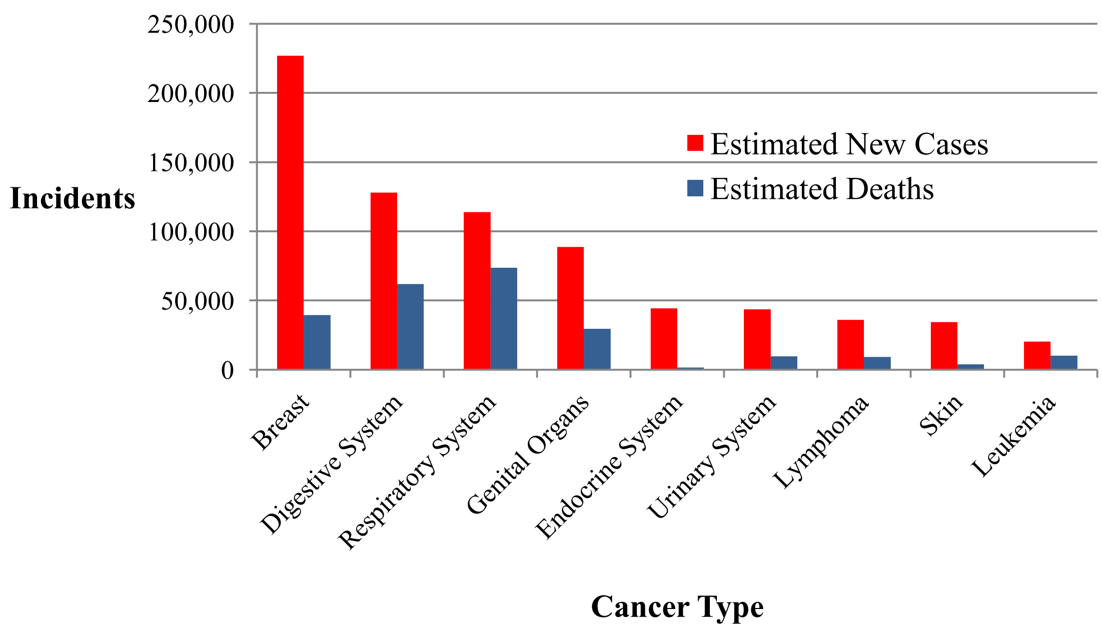

Figure 1-1: 2012 estimated new cases of cancer and deaths from cancers from ACS.

Breast cancer is the most prevalent cancer for women with an estimated 226,870 new cases in 2012 ((ACS), 2012). While the prevalence is high, the mortality is relatively low, with an estimated 29,510 deaths from breast cancer in the same year. Comparing that to digestive system cancers, which has 61,950 deaths for 127,920 incidents, the relative pervasiveness and mortality comes into perspective. In the course of a woman's lifetime, their chance of getting breast cancer is 14.90%. For those who get cancer and then receive treatment, recurrence-free survival rates were 89% and 80% at 5 and 10 years, respectively (Brewster, et al., 2008). With these figures in mind, it is clear that research into new breast cancer treatments is crucial in order to further lower the mortality rate and increase the recurrence-free survival rate.

1.1 Treatment of Breast Cancer

Treatment of breast cancer varies depending on the individual cancer's classification, especially concerning the tumor size, spread, and risk of recurrence. Protocols have been published that recommend specific treatment regimens for breast cancers that fall into specific categories. There are three categories of treatments which may generally fall under: surgery, systemic (chemotherapy and hormonal therapy), and radiation therapy.

1.1.1 Surgery

Surgical removal of the tumor is recommended for nearly all cases of breast cancer with several exceptions for low risk cancers.

A mastectomy is recommended in cases where more than one tumor exists, the breast has been previously radiated, the tumor is large relative to the size of the breast, the patient has a complicating disease, the patient lives in an area inaccessible to radiotherapy, or the patient opts for the treatment. A traditional mastectomy removes all the breast tissue from one or both breasts, with nearby lymph nodes removed as well.

Variations of this procedure may be used in order to spare skin or nipple or to remove nearby muscle.

Contrasting the mastectomy, a lumpectomy only removes a small portion of the breast and may be used in cases for patients with small, lower risk cancers that have not metastasized throughout the body (Wazer, et al., 2006). It is considered breast conserving therapy (BCT) and has the advantages of superior cosmetic results, and reduced psychological and emotional trauma (Bartelink, et al., 1985). The disadvantages include greater complexity, longer treatment, and potential logistic problems. However, for lesions smaller than 4cm, lumpectomy techniques have been found to be as effective as mastectomy (Morris, et al., 1997).

Removal of lymph nodes in the axilla is considered. Currently sentinel lymph node removal is the standard of treatment, which removes a few nodes, whereas removal of 10-40 nodes was the previous standard of treatment. Removal of many lymph nodes however, can lead to lymphedema. Lymph nodes and lumpectomy excisions are tested for cancer to ensure clear margins. The number of positive lymph nodes may contribute to the choice of other treatments with more aggressive treatments for more distributed diseases.

1.1.2 Systemic Therapies – Chemotherapy and Hormonal Therapy

Systemic treatments can be given depending on the characteristics of the cancer and the treatment goals. These treatments may be given neoadjuvantly, in order to reduce the size of the tumor before surgery, adjuvantly, given after surgery to reduce recurrence risk, or palliatively, in order to control cancer when it has spread beyond the breast, or a combination of these.

There are many chemotherapy regimens that may be chosen depending on the characteristics of the tumor, lymph node status and age and health of the patient. For example, doxorubicin and cyclophosphamide is commonly given in cases where the cancer has not spread to lymph nodes.

Hormonal treatment can target certain hormones if at elevated levels in breast cancer. Estrogen will promote cancer growth when estrogen or progesterone receptors are present in certain breast cancers. In order to combat this, anti-estrogen drugs like tamoxifen and toremifene are administered. These block the estrogen from binding to their receptors, and stop the growth signal from reaching the cancer cell.

1.1.3 Radiation Therapy

Radiation therapy's purpose is to reduce the risk of recurrence by limiting the ability of the remaining, occult tumor cells to reproduce. Generally, it is used as an adjuvant therapy after a patient has undergone a lumpectomy and, in some cases, a mastectomy. A BCT regimen of radiation therapy after lumpectomy has been shown to be as effective as mastectomy for stage I and II breast cancers (Veronesi, et al., 2002) (Fisher, et al., 2002). Superior cosmetic results and reduced trauma are associated with BCT compared to mastectomy. The disadvantages of BCT include increased treatment time and complexity of treatment due to the course of radiation therapy. BCT has traditionally included whole breast irradiation (WBI) after a lumpectomy has been performed. The common WBI administration was to treat the entire ipsilateral breast with tangential fields for 5 weeks with additional 2 week of daily radiation boost to the tumor bed. This would ensure that all the breast tissue would be dosimetrically covered and any occult disease would be removed.

The justification for whole breast radiation has been brought into question by studies which have found that the majority of recurrences occur near the original tumor bed (Fisher, et al., 2002) (Veronesi, et al., 2002) (Clark, et al., 1996) (Holli, et al., 2001) (Lilijergren, et al., 1999), and ones that have found that the rate of recurrence after surgery in the ipsilateral breast without irradiation was very similar to the contralateral breast at 13% and 10%, respectively (Smith, et al., 2000).

The results of these studies illustrate that partial breast irradiation (PBI) is a legitimate alternative. Conditions of eligibility for PBI have been developed by the Radiation Therapy Oncology Group (RTOG) in order to ensure effective treatment (Vicini, et al., 2005). These conditions include patients with Stage 0, I, or II breast cancer that has been resected by lumpectomy, that their tumor was ≤ 3.0 cm, and they have no more than 3 histologically positive nodes. The advantage to PBI is the ability to have a much shorter treatment time, reducing the nearly 2 month treatment of WBI to less than 2 weeks; when shortened to this timetable, it is considered accelerated partial breast irradiation (APBI). Several variations of PBI have been used clinically.

Interstitial breast brachytherapy uses a series of catheters placed within the breast through the lumpectomy cavity. Initially it was used as a low dose rate (LDR) procedure delivering 50 Gy to the patient over 96 hours. With this procedure a 0.9% 5-year rate of recurrence was produced with good to excellent cosmetic results were judged in 91% of patients (Vicini, et al., 1999) (Vicini & Chen, 1997). High dose rate (HDR) has also been used with this technique to deliver 34 Gy in 10 twice-daily fractions over 5 days. In-breast recurrence rates using this technique were 3% (Arthur, 2008).

Another form of partial breast irradiation exposes the lumpectomy cavity to radiation during the surgical excision procedure - intraoperative radiation therapy (IORT). Once blood loss has stopped, a spherical applicator is inserted into the cavity, with a radiation-emitting source in the sphere. The dosimetry in the breast may be adjusted by using shielding created during the procedure. The source is turned on for 21 to 28 minutes in order to deliver 5 Gy. Vaidya *et al.* reported no recurrences after a short median follow-up of 24 months. Another more conventional form of IORT is what is known as the Electron Intraoperative Radiation Therapy (EIORT), which in addition to being used for partial breast irradiation (Figure 1.2), is used as an adjuvant to surgery and/or fractionated external beam radiation therapy for locally advanced cancers of the abdomen, pelvis, neck, cranium, thorax and extremities (Dobelbower, et al., 1989). At present, EIORT and orthovoltage IORT, with typical energies around 250 kVp, are also competing modalities to SAVI system and Balloon catheters used for delivering radiation to malignant tissue during surgery.

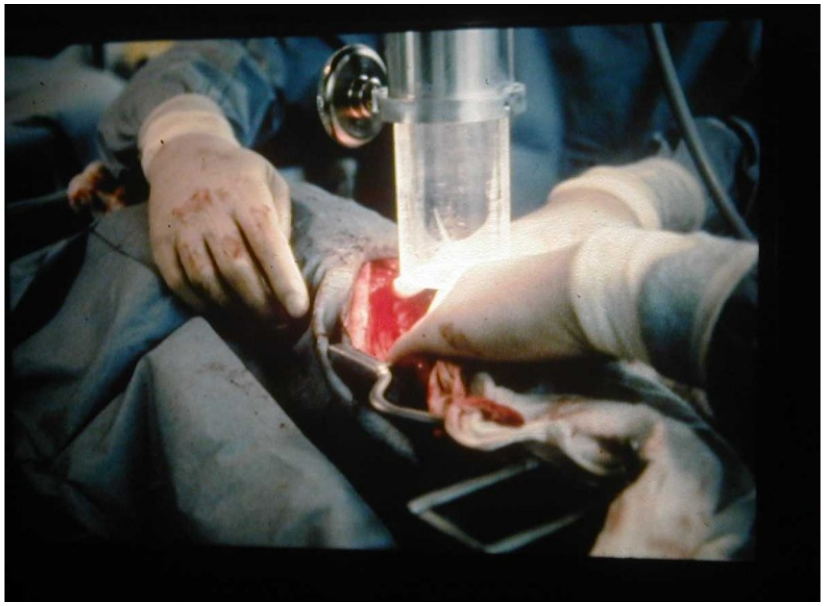

Figure 1-2: —Intraoperative radiation therapy setup for a patient with breast cancer at the University of Toledo Medical Center, 2003.

3D conformal external beam radiation therapy incorporates the use of several beams from a linear accelerated aimed at a target defined as the tumor cavity plus a 2 cm margin (Formenti, et al., 2002). 5-6 Gy per fraction in five fractions was used in this scheme. A median follow-up of 24 months for 91 patients treated with this technique found no local recurrence (Vicini, 2007).

Intracavitary catheter brachytherapy was introduced in response to some of the disadvantages presented by other modalities, including complexity, unavailability of treatment machines in operating rooms, and surrounding tissue toxicity. The first device introduced was the MammoSite balloon in 2002, seen in figure 1-~~2~~3. It has a catheter that can be attached to an HDR afterloader to input the source. The end of the catheter is surrounded by balloon of diameter of 4 to 5 cm that can be filled with saline or contrast solution. The balloon is implanted into the lumpectomy cavity where 34 Gy can be delivered in 10 fractions of 5 days prescribed to 1 cm from the applicator surface. The advantages to the MammoSite are its ease of use, only being a single entry device.

Figure 1-3: The MammoSite (www.MammoSite.com).

Certain additional criteria must be met for this treatment to be available to a patient. The cavity must be at least 3 cm in 1 dimension and it is important to have at least 1 cm balloon-skin spacing (allowing 5 mm or more for up to 3 CT slices of 3 mm thick) to allow for skin sparing. Because of these criteria, a number of patients who are planned for a MammoSite may not meet eligibility to receive this treatment. The MammoSite cannot produce a dose that conforms to the anatomy of the patient. Dose asymmetry is impossible due to the geometry of the MammoSite; the dose will always be radially symmetric and adjustment of dwelling times may only create elliptical isosurfaces, but yet symmetric along the catheter's length. More than 20% of patients were ineligible for this treatment due to small cavity size, small balloon-skin spacing, or other criteria in a study by Benitez *et al.* (Benitez, et al., 2007). Recurrence rates for those treated with MammoSite however, were similar to WBI at 1.6% at 5 years (Vicini, et al., 2007). The criteria mentioned above is used to limit the dose to the skin, however even when these criteria are followed, large skin or chest wall doses may occur which can lead to chronic pain and rib fracture (Brown, et al., 2012) (Cuttino, et al., 2009) (Brashears, et al., 2009).

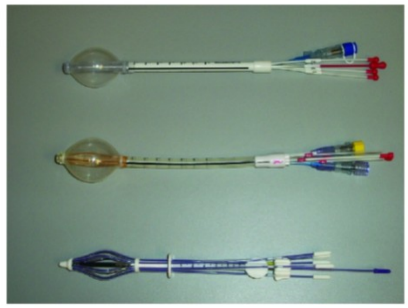

Figure 1-4: Three intracavitary breast brachytherapy applicators. Top: MammoSite. Center: MammoSite ML. Bottom: SAVI. (openi.nlm.nih.gov)

Multi-lumen devices similar to MammoSite have been introduced to allow for asymmetric dose distributions. MammoSite-ML is nearly the same as the MammoSite except for the addition of 3 lumens to surround the central lumen in 120° intervals. The Contura applicator has 4 evenly spaced lumens surrounding a central lumen. Both of these have the lumens contained within a balloon of radius 4-6 cm. Rotation needs to be limited in these applicators to ensure proper treatment. The peripheral lumens are placed very close to the central lumen for these applicators, only being 2mm away for the MammoSite ML and 5mm away for the Contura. This inherently limits the applicators' ability to produce asymmetric dose distributions.

Cianna Medical's Strut-Adjusted Volume Implant (SAVI) uses a different design concept than the balloon applicators. Rather than a balloon surrounding several lumens, 6-, 8-, or 10- struts are positioned around a central lumen. Once within the breast, the struts are expanded, which in turn expands the cavity. This cavity is initially filled with air but over the course of treatment may fill with seroma. Because no balloon is present, no contrast fluid can be inserted into the cavity, however the applicator and tissue can be clearly seen in CT images taken of the SAVI within the breast.

For all of these applicators, source weighting (dwell times) in each lumen can be adjusted to produce asymmetric dose distributions. However, because of the different nature of SAVI compared to balloon applicators, it allows for greater dose asymmetry, and allows more patients to be eligible for APBI. In a study of 102 patients using SAVI, 27% were not eligible for MammoSite, and 5% were not eligible for any balloon brachytherapy (Yashar, et al., 2009).

Table 1-1: Results from Scanderbeg et al. of several pertinent volumes for 3 APBI techniques. Notice SAVI has lowest dose CW/rib, lung, and skin.

	PTV Volume (cc)	V90	V150 (cc)	V200 (cc)	CW/rib	Lung	Skin
SAVI	59.9	97.70%	25	10.4	75.00%	64.70%	51.50%
MammoSite	71.5	97.60%	23.9	5	100.00%	75.00%	95.00%
3D-CRT	351.6	100.00%	N/A	N/A	105.30%	93.80%	104.00%

Scanderbeg *et al.* (Scanderbeg, et al., 2009) studied the effect of dose asymmetry using SAVI and comparing it to MammoSite and 3D conformal radiotherapy, results can be seen in Table 1-1. It is apparent that SAVI has the greatest normal tissue sparing capability, getting the average chest wall, lung, and skin dose down to 75.0%, 64.7%, and

51.5%, respectively, compared to MammoSite's 100.0%, 75%, and 95% and 3DCRT's 105.3%, 93.8%, and 104.0%.

SAVI's dosimetric flexibility presents unique possibilities for candidates of APBI.

1.2 Brachytherapy Dosimetry

Being able to properly predict dosimetry is crucial for effective treatment using radiation. In a study of prostate cancer, D_{90} was found to be an independent predictor for recurrence-free survival (Zelefsky & Whitemore, 1997). Other studies have found that only D_{90} affected recurrence free survival and other factors such as patient age, radionuclide selection, and use of teletherapy had no affect on this. Clearly, effective brachytherapy treatment depends on accurate dosimetric planning.

The earliest brachytherapy dosimetry used tables based on measurements and Sievert integrals, while the current standard of care has been to follow the American Association of Physicists in Medicine (AAPM) Task Group No. 43 (TG-43) updated report (Rivard, et al., 2004). Initially published in 1995, TG-43 called for the use of air-kerma strength (S_K) in order to calculate dose rate in the following general equation:

$$\dot{D}(r,\theta) = S_K \wedge \frac{G_L(r,\theta)}{G_L(r_0,\theta_0)} g_l(r) F(r,\theta).$$

Air-kerma strength is the measure of a source's strength in terms of its air-kerma rate for a small mass of air in vacuum at a distance. Reducing uncertainties in measuring this unit for sources has been pursued throughout its use. $\wedge$ is the dose-rate constant, defined as the dose rate per unit air-kerma strength at a point along the transverse axis of the source. G_L is a line source dose approximation and accounts for the effect of the distribution of radioactive material inside a source. g_l is a radial dose function and accounts for the attenuation of radiation in tissue. Finally, F is a 2D anisotropy function, and corrects for affects from the source and capsule on the dose distribution. TG-43 formalism replaced calculations that were based upon apparent activity, equivalent mass of radium, exposure-rate constants, and tissue-attenuation coefficients. It accounts for differences between sources like encapsulation or internal construction; where-as other formalisms did not.

The introduction of TG-43 was a major advance to brachytherapy dosimetry. It introduced a standardized method for dosimetry that allowed dose uncertainties of less than 5%. However, TG-43 has inherent issues that have plagued brachytherapy dosimetry throughout its history. Thomadsen *et al.* reviewed past and current issues affecting brachytherapy in 2008 (Thomadsen, et al., 2008). Of these, accounting for heterogeneities is one of the most difficult issues to overcome. Heterogeneities may arise from various sources, such as differences in tissue, presence of applicators, and intersource shielding. TG-43 assumes that radiation will traverse through water to deliver a dose to water with full backscatter. This is not the case for actual patients and this assumption can lead to dosimetric inaccuracies and underdosing. A study using MammoSite measured the difference in dose to tissue near the breast-air interface to tissue near the breast-lung interface and found a dose reduction of as much as 14.8% and 6.2% for Yb-169 and Ir-192 sources, respectively (Cazedca, et al., 2010). A mean dose reduction of 6% and maximum 12% was found from interseed effects (Meigooni, et al., 1992). In a replication of an esophageal brachytherapy treatment, doses were overestimated by 10% to the trachea wall (Uniyal, et al., 2013). For certain treatments involving relatively homogeneous tissue, the effects of heterogeneities can be ignored with little impact, one study finding <2.2% dose difference to bladder, rectum, and point A for tandem-and-ovoid treatment (Hyer, et al., 2012). However, even for cases with small differences, accounting for heterogeneities can assist in better treatment planning and can lead to better clinical results.

The use of a more robust dose calculation algorithm can account for the affect of heterogeneities. External beam therapy has used heterogeneity corrected calculations for many years by use of model-based dose algorithms that explicitly simulate the transport of radiation in actual media or employ multiple dimensional scatter integration techniques to account for the dependence of scatter dose on the three dimensional geometry. These techniques include collapsed-cone superposition/convolution method, which uses the approximation where all energy inside a specified solid angle will be transported along a line. Another finds a deterministic solution using the linear Boltzmann transport equation. A third technique uses Monte Carlo simulations which repeatedly performs the transport of a particle using probabilities to calculate a final result.

The AAPM's Task Group 186 (Beaulieu, et al., 2012) reports on model-based dose calculation methods (MBDCA's) for brachytherapy and their use in practice. It addresses three issues specific to MBDCA's. The first is the dose calculation medium of which there are three scenarios: dose through water to water, dose through heterogeneous medium to heterogeneous medium, and dose through heterogeneous medium to water. The report recommends that the transport of radiation be performed through heterogeneous medium and the dose is calculated to local medium, which can then be compared to TG-43 calculated doses. The second issue concerns voxel cross section assignments. Current methods of obtaining information on treatment media, such as single-energy CT, do not provide adequate guidance in these assignments. TG-186 recommends that a set of standardized materials be used in order to ensure uniformity through all institutions. An MBDCA commissioning procedure is the last issue TG-186 addresses. A two part procedure is suggested consisting first of reproducing TG-43 dose parameters and then testing the capabilities of the MBDCA to account for advanced clinical scenarios.

1.3 Monte Carlo Simulation for Brachytherapy

Monte Carlo methods involve the heuristic technique of using large numbers of repeated random sampling to derive a result. This process contrasts deterministic models where the outcome is known from the beginning. Monte Carlo simulations are necessary with complicated problems where deterministic methods are impossible to utilize. They were first used in nuclear weapons problems in Los Alamos National Laboratory in the 1940's. As this method matured, it was adopted for use in radiation therapy.

In 1971, Monte Carlo (MC) calculations were first used to predict the dose distribution from Californium-252 needles in tissue (Krishnaswamy, 1971). Due to the heuristic nature of MC simulations, they can be time consuming and sample constraining. As such, in early MC simulations, histories on the order of 10^3 were performed. The number of histories performed has increased exponentially with the increase in computing power since then with 10^{10} histories now being applied to MC simulations (Paixao, et al., 2012). Brachytherapy is used in medical physics to examine a variety of problems including modulated proton beams (Farr, et al., 2013), EPID backscatter (King & Greer, 2013), and shielding for IMRT (DeMarco, et al., 2013).

In the 1990's, Monte Carlo use for brachytherapy dosimetry significantly advanced with TG-43 mentioning the possibilities of its utilization. Several Monte Carlo transport codes are available to be used such as EGS, MCNP, PTRAN and GEANT4. MCNP5 (Los Alamos National Laboratory, Los Alamos, NM), abbreviated from Monte-Carlo N-particle, is the transport code to be used in this study. Developed in Los Alamos National Laboratory, it is capable of using three-dimensional geometry to model the transport of neutrons, gamma rays, and electrons. Individual particles are tracked from their sources one at a time. As a particle travels through material, various interactions may occur at a rate determined by a probability distribution. These interactions may produce other particles or transfer some energy to the location. Once the particle loses all of its energy, it reaches an endpoint. The program then similarly tracks the transport of each created particle. Once it runs through all of these, it will start again with another particle originating from a source. This process will repeat until the desired number of particles is simulated. Tallies can be created to measure an assortment of different calculations such as surface current, average surface flux, and energy deposition. Once the simulation is completed, an output file is created with various statistics from the calculation and results of the tally measurements.

1.4 Purpose

Inherent heterogeneities exist for SAVI creating unique dosimetric issues for treatment planning systems. Being an APBI device, the SAVI will be near tissue-air and tissue-lung interfaces, which alters the amount of backscatter contribution to the planning treatment volume (PTV). In a study of the Contura, a dose decrease of approximately 5% was found when no backscatter material was present compared to full backscatter (Williams, 2012). The effect on the SAVI may be different due to disparity in the geometries of the two devices. SAVI's ability to produce a high level of asymmetry may also affect the backscatter contribution.

When the SAVI is inserted into the lumpectomy cavity and the struts are extended an air cavity is created within the struts. As time goes by, serous fluid may fill the cavity. Dosimetrically, the contents of this cavity should make some difference.

TG-186 states that uncertainties in tissues affect the dosimetry in brachytherapy implants (Beaulieu, et al., 2012). Breast tissue is a mixture of adipose and glandular tissue, the proportion of which is different from woman to woman and may change over time. This composition is different from water. Differences in composition affect dosimetry.

In this thesis, the affects of these heterogeneities will be studied using MCNP. Similar previous studies have been done on the Contura (Williams, 2012) and with the SAVI (Richardson & Pino, 2010). The former study investigated the affect of the amount of backscatter material on the dosimetry around the Contura and will be discussed further below. The latter study focused on the affect of the contents of the cavity within the SAVI and found a dose increase when the cavity was filled with air rather than water. This dose increase was more apparent when the average distance travelled through the cavity by the photons was higher such as when the sources are weighted more in the outer lumens. Similar to the Williams study, Dose modification factors (DMF's), defined as the dose with full backscatter divided by the dose at another point (Kassas, 2006), will be calculated from the obtained MCNP data. Relative doses will also be compared between the trials. Finally this data will be compared to similar plans created in BrachyVision in order to test the validity of both its TG-43 dose calculation algorithm and its Acuros dose calculation algorithm.

Chapter 2

Materials and Methods

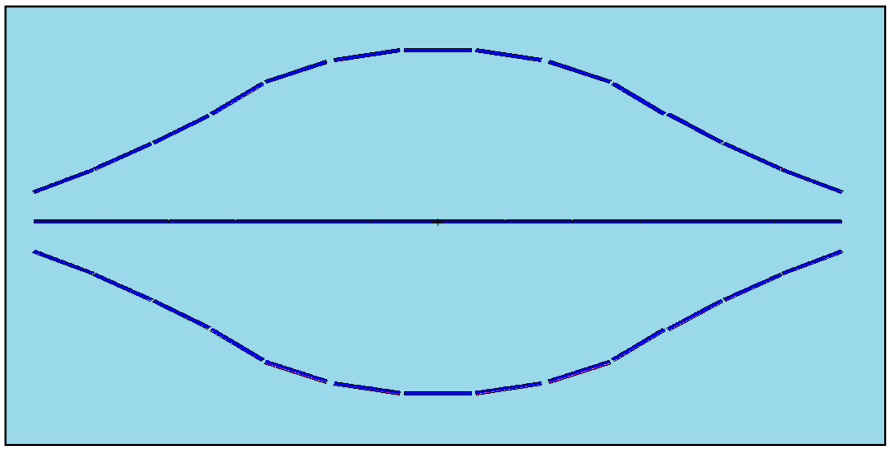

Figure 2-1: Schematic of SAVI model. Image from Vised.

A model of the SAVI based on measurements of the physical device was created for MCNP5, see Appendix A. This model was based on work done by Makenzie Enders in the 2012 REU program at the University of Toledo.

For these simulations several reasonable assumptions were made. The sources are all present at the same time, rather than the physical reality of a single source dwelling at specific positions in a single lumen at a time. Having the sources present adds attenuating material not actually present in the clinical setting. However, this affect is insignificant and can be ignored (Williams, 2012). The wire was also excluded from this model. It has previously been found that the presence of the wire has little effect on the final results of these types of studies (Williams, 2012).

The central lumen of the applicator consists of 12 sources aligned along the x-axis, centered at the origin. Eight lumens were symmetrically placed around the central lumen. Each of these lumens has 13 sources placed in positions that correspond to the measured SAVI applicator. Figure 2-1 demonstrates the schematic for the SAVI. As mentioned previously, all sources are present during the simulation, so source weighting is adjusted to give the desired dose distribution, rather than a source dwelling at a position for a period of time. Source weighting was found by normalizing dwell times from BrachyVision (BV, Varian Medical Systems, Inc., Palo Alto CA) treatment planning system. For less than 1% uncertainty at the tally placed 1 cm away from the SAVI, 2 x 10^7 histories needed to be performed. The f6 tally, which records energy deposition in MeV/gm, was used for all tallies.

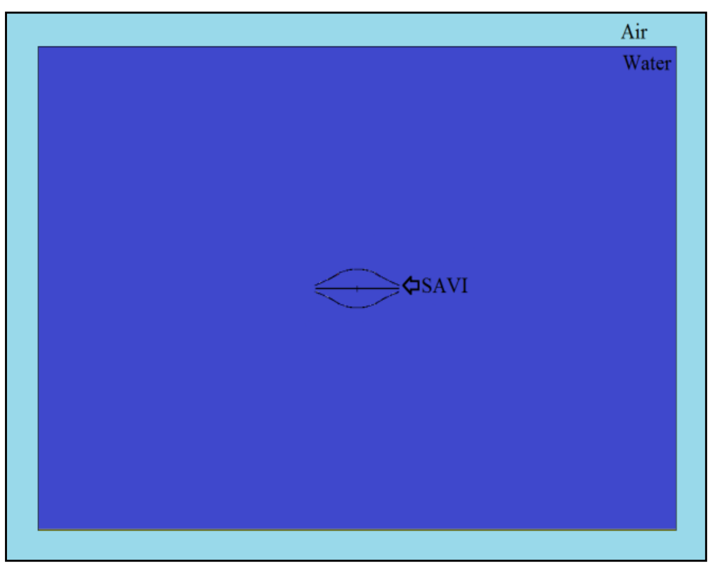

Figure 2-2: Base plan of SAVI MCNP trials.

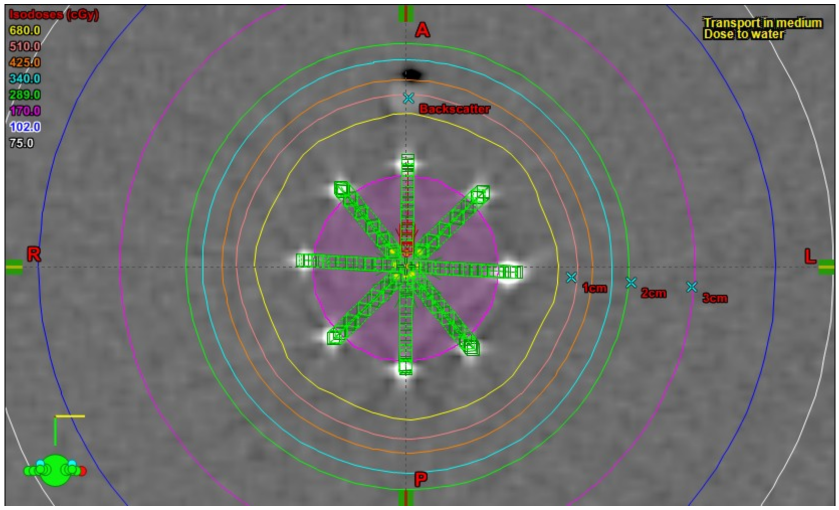

Figure 2-3: Symmetric dose distribution from SAVI plan in BrachyVision.

The base plan consisted of the SAVI placed at the origin with a cubic water phantom with sides of 45.6 cm placed around it, see Figure 2-2. The position of the SAVI in the middle of this large phantom allowed for full backscatter. Outside of this was a cube of air with sides of 100 cm. If particles reached beyond this, they were not tracked any longer. The sources were initially weighted for a symmetric plan as found by BrachyVision (See Figure 2-3).

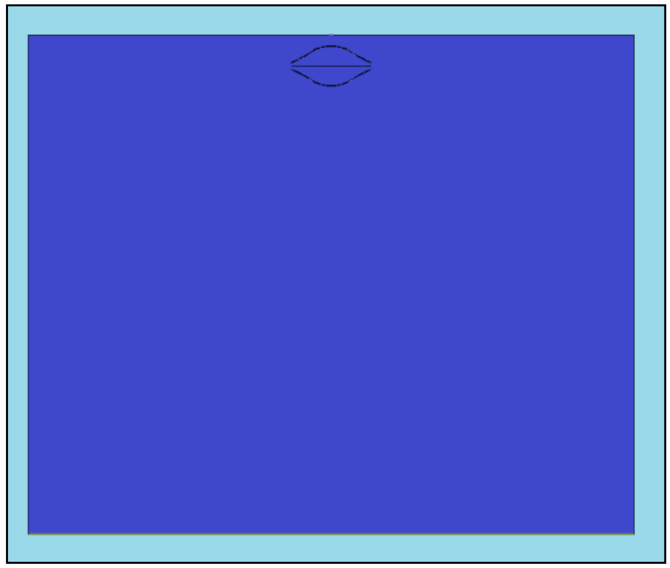

Figure 2-4: Image demonstrating SAVI closer to water-air interface through movement of cubic phantom. This image shows water-air interface at 1cm away from applicator. Trials were run at several intermediate positions from applicator at center (see figure 3-2) to measure affect of backscatter.

In order to test the affect of backscatter, different trials were run with the water-air interface being adjusted at 1cm increments starting at 1cm away from SAVI, for no backscatter, to the base 20cm away, for full backscatter, shown in figure 2-4. A simulation was also always done with the water-air interface at 1.5cm away from the applicator. The water phantom's position moves in the z direction to adjust this, without ever changing its size.

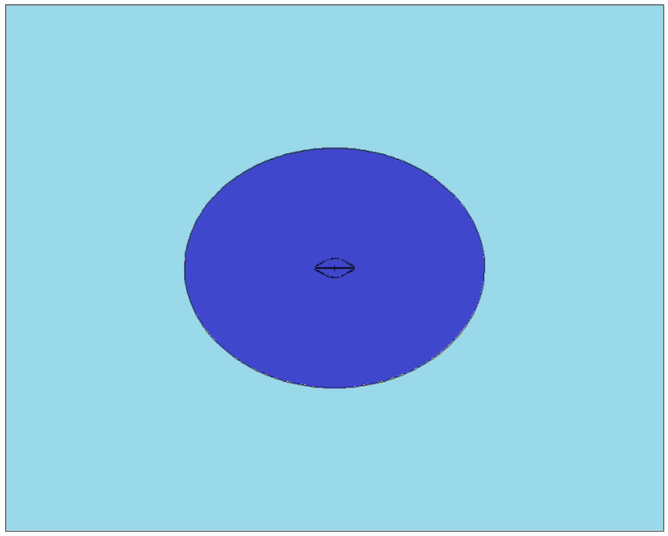

Figure 2-5: Image of second experiment - the spherical phantom.

In the second experiment, a sphere of radius 22.8 cm (see Figure 2-5) was used rather than a cube with similar backscatter tests carried out.

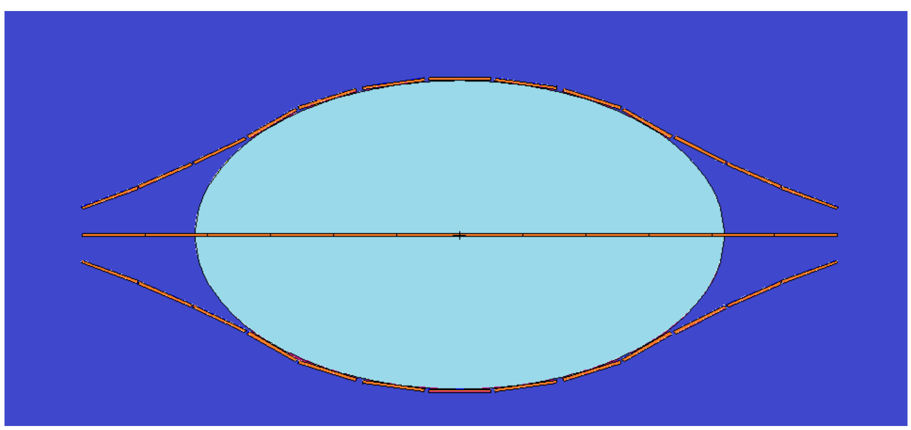

Figure 2-6: Light blue show ellipsoid cavity created within SAVI applicator for third experiment.

The third experiment place an ellipsoid air cavity within the SAVI rather than water to simulate when air is contained within the cavity created by the struts rather than seroma, see figure 2-6. A number of simulations were done varying the amount of backscatter material, similar to the base trial.

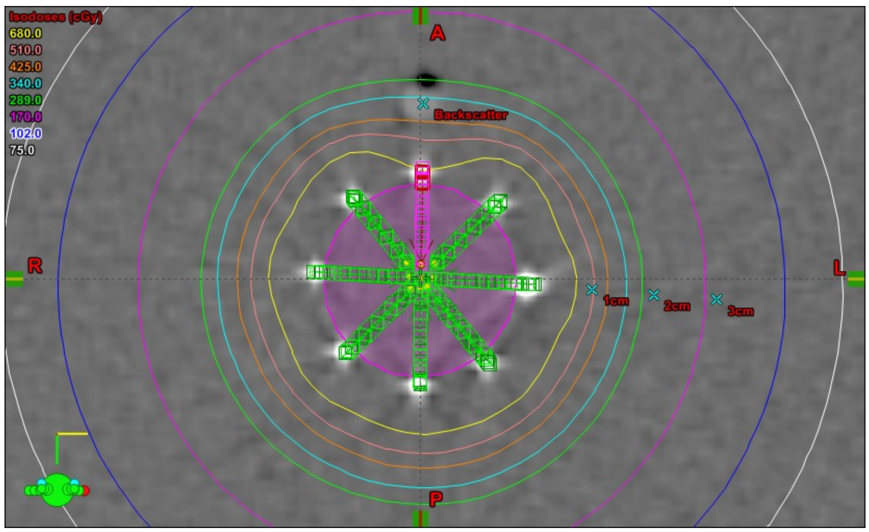

Figure 2-7: Asymmetric plan for SAVI derived from BrachyVision. Refer to Figure 2-3 for comparison.

The fourth experiment used source strengths derived from an asymmetric BrachyVision plan (See figure 2-7). This created a plan with the opposite lumen from the tally with zero weighting.

Table 2-1: Composition specifications.

Tissue	% mass				Mass density
	H	C	N	O	g/cm^3
Adipose	11.4	59.8	0.7	27.8	0.950
Glandular	10.6	33.2	3.0	52.7	1.020
Average	11.0	46.5	1.9	40.3	0.985
Water	11.2	0.0	0.0	88.8	1.000

The final experiment changed the composition of the water phantom from water to the composition of breast tissue taken from Woodard *et al.* (Woodard & White, 1986), shown in Figure 2-1.

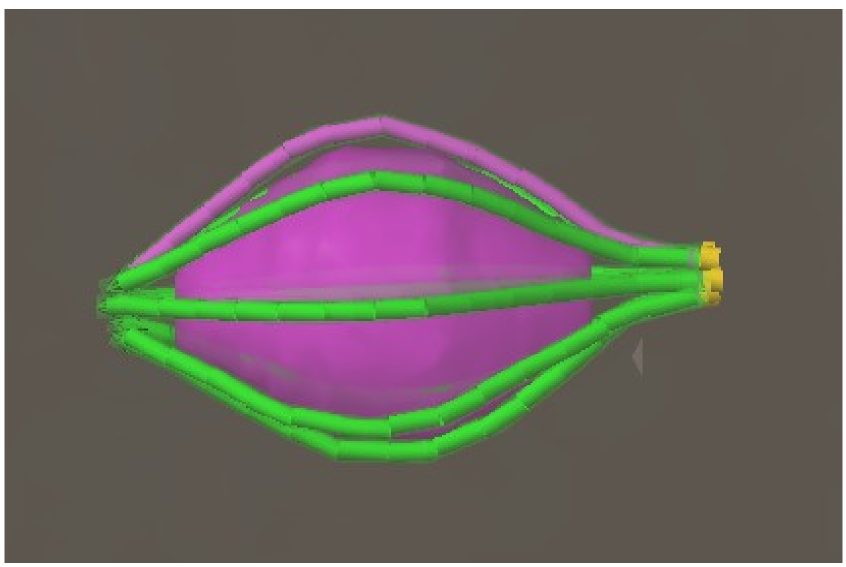

Figure 2-8: 3D representation of SAVI model used in BrachyVision tests.

For comparison, plans were made on BrachyVision and doses were calculated using both their TG-43 and Acuros dose calculation algorithms and for both symmetric and asymmetric plans, with both air and water in the cavity

Chapter 3

Results and Discussion

3.1 Model Validation

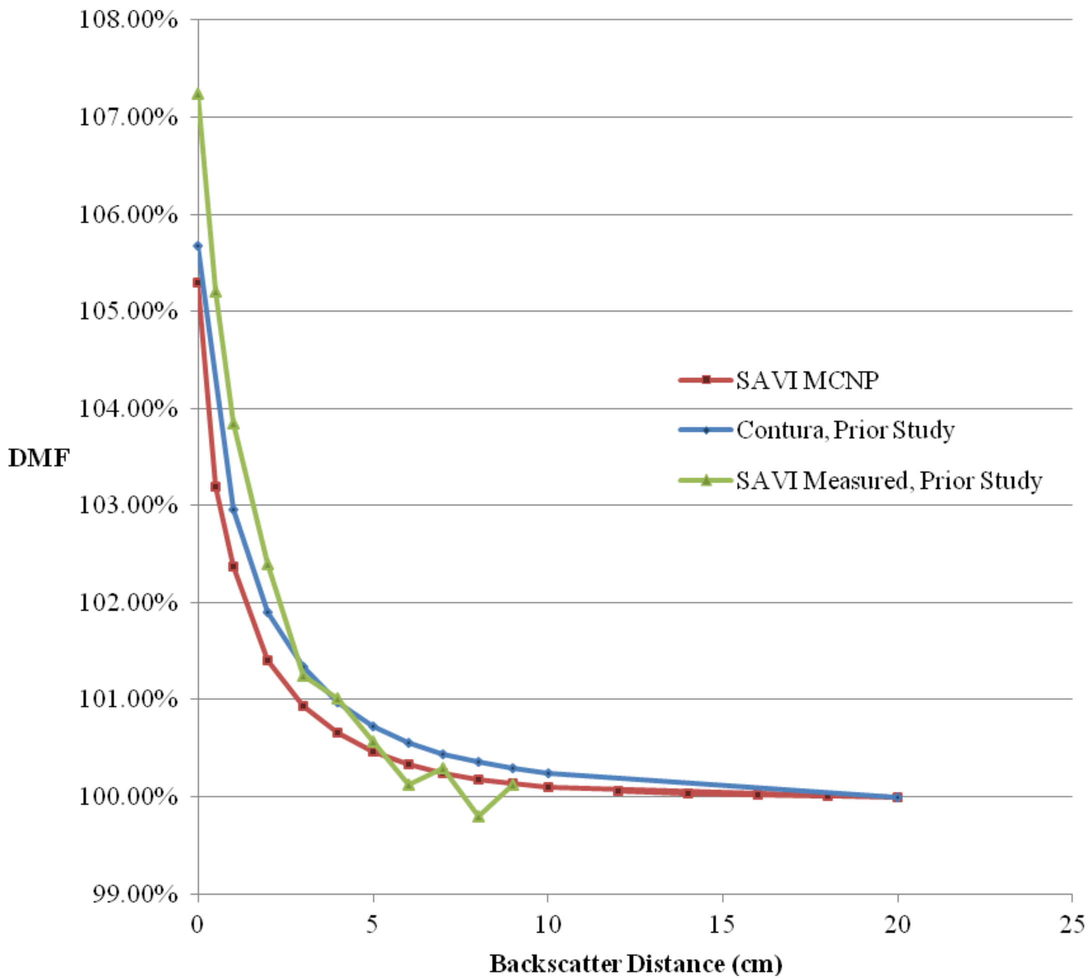

Figure 3-1: Dose Modification Factor (DMF), defined as the dose with full backscatter divided by the dose at another point (Kassas, 2006), comparison of MCNP simulation of SAVI, previously MCNP simulation of Contura (Williams, 2012), and physically measured SAVI (Sherman, 2011).

DMF’s were compared to those found from an MCNP study of the Contura (Williams, 2012) and a physical study of the SAVI (Sherman, 2011), see Figure 3-1. Both the Contura and SAVI were simulated in a large cubic water phantom and brought closer to the water-air interface to measure the backscatter contribution from 0-20 cm. The physically measured SAVI was placed in a rectangular phantom, and was measured from 0 to 10cm. The Contura and SAVI MCNP results are similar (<1% difference), thus providing a validation that our model was reasonable.

The measured SAVI data is considerably different. This could be due to the difficulty in setup and measurement for a physical applicator compared to the easily controllable environment of the simulation. Because physical measurements were not taken under full backscatter conditions, the physical values were normalized to 100.13% for 9cm, matching the measurement for the MCNP model. Even with this assumption made in order to account for the difficulty of measurement, the physical DMF’s are nearly 2% higher with little backscatter material and have a steeper decrease with more backscatter material added. Discrepancies between MCNP simulations and physical measurements should be disregarded due to the lack of consistency and difficulty of measurement of the latter.

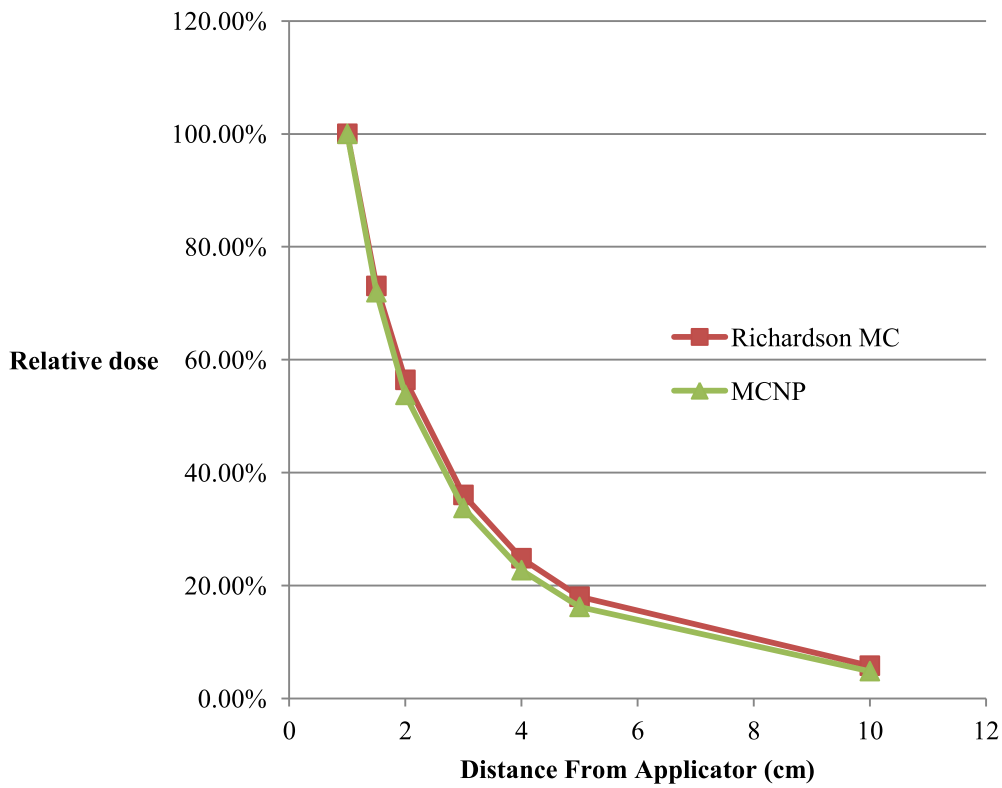

Figure 3-1: Comparison of MCNP data with previous Monte Carlo study.

The model was also compared to a previous Monte Carlo study of the SAVI (Richardson). For this validation, only the center dwell position was used in the central lumen. Relative doses were found at distances between 1 and 10cm. Results, presented in Figure 3-2, were nearly identical, with less than 2% difference, which can be expected from differences in each model.

With the model validated through comparisons to previous studies, other studies could be performed.

3.2 Effect of Backscatter

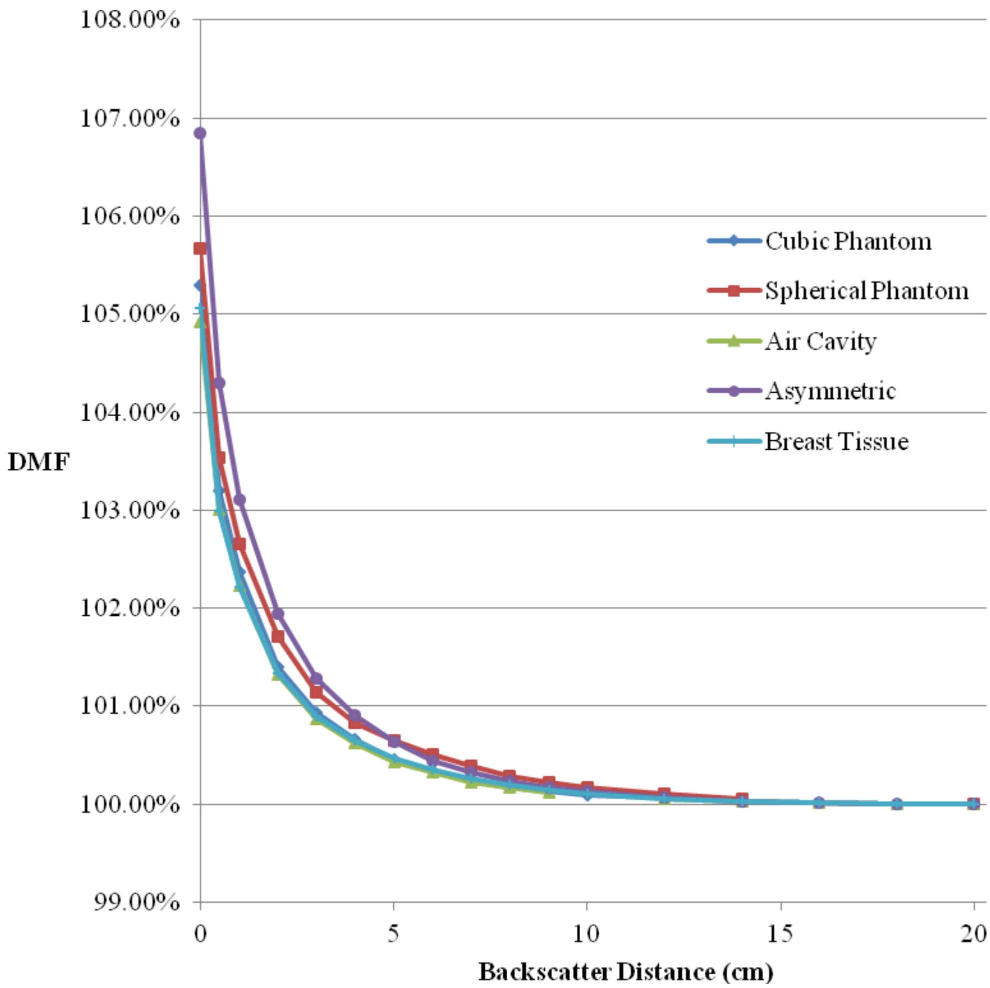

Figure 3-3: Comparison of DMF's found by MCNP for five trials.

Dose modification factors (DMF's) were calculated for each trial and presented in Figure 3-2. It is apparent that the amount of backscatter contribution for each case is very similar, with approximately 5% dose reduction occurring when no backscattering media is present for all cases. The asymmetric plan was most affected by the lack of backscatter having nearly a 2% greater dose reduction. The sphere trial was affected by the lack of backscatter because of the smaller amount of backscattering media for a sphere of radius 22.8cm compared to a cube with sides of 45.6cm. The contents of the cavity and composition of backscattering material each had little effect on the DMF compared to the symmetric plan with a water cavity surrounded by water.

3.3 Relative Dose

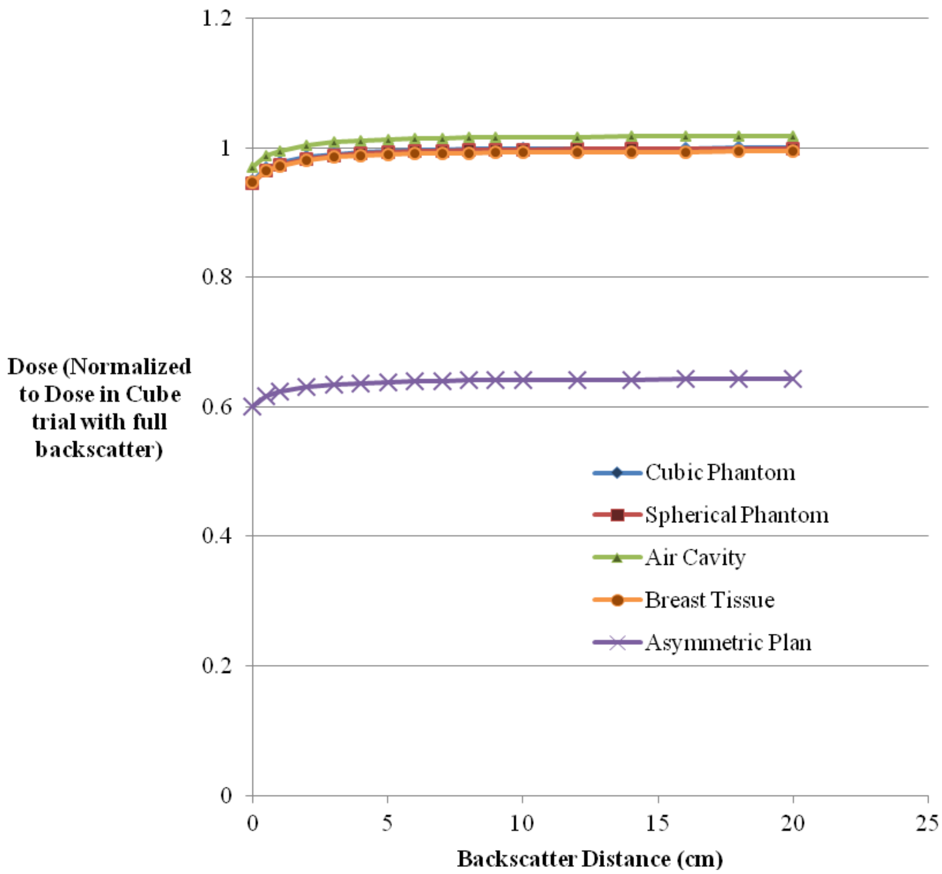

Figure 3-4: Relative dose for five trials. Doses are normalized to the cubic phantom in full backscatter conditions. Note dose reduction in asymmetric plan.

Doses to a point 1cm away from the SAVI for each trial normalized to the dose in the base trial (cubic, symmetric, water cavity, surrounded by water) at 20cm are presented in Figure 3-3 and 3-4. From figure 3-3, SAVI's ability for dose asymmetry is apparent, reducing the dose to approximately 60% of the symmetric dose. Figure 3-4 shows only four trials in order to present the data from those trials more clearly.

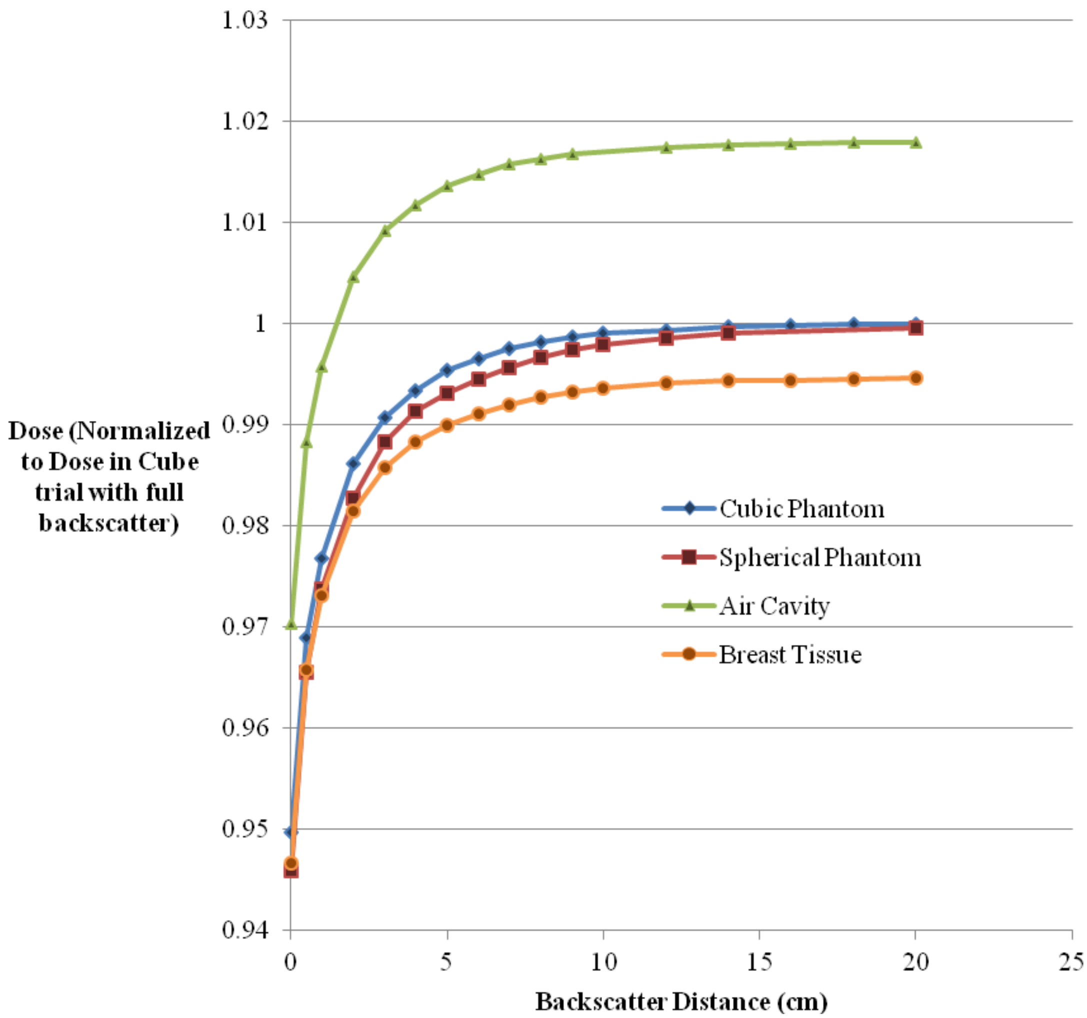

Figure 3-5: Relative dose for four trials. Doses are normalized to the cubic phantom in full backscatter conditions.

Doses were very similar between the cube and sphere trial especially as the amount of backscatter material increased.

The air cavity trial also presented a higher dose of a maximum amount of 2.17% with a backscatter distance of 0 cm. There is less attenuating material between sources and the tally in this trial, especially for the lumens on the opposite side of the SAVI from tally. This accounts for the higher dose in this trial.

Composition had a slight effect by decreasing the dose by an average of 0.50%. Water and average breast tissue have a very similar composition and so produce a similar dose distribution.

3.4 Cavity Contents, Comparison to Treatment Planning System Dose Calculation

The effect of changing the cavity media for an asymmetric and symmetric plan was also studied, see Table 3-2.

Table 3-1: Results of MCNP simulation of SAVI with air- and water-filled cavity with symmetric and asymmetric plan. Doses were found at 1, 2, and 3 cm away from the applicator. Doses were also found using BrachyVision treatment planning system (TPS) using its TG-43 protocol calculation algorithm (BV-TG43) and Acuros model-based dose calculation algorithm (BV-Acuros). Differences between MCNP air- and water-filled cavity trials were found and between BV-TG43 and BV-Acuros.

		Symmetric Plan			**Asymmetric Plan**		
MCNP	*Distance (cm)*	*Water*	*Air*	*Difference*	*Water*	*Air*	*Difference*
	1	98.23%	100.00%	1.77%	87.01%	100.00%	12.99%
	2	48.64%	49.49%	0.85%	58.61%	66.39%	7.78%
	3	30.85%	31.35%	0.50%	42.47%	46.99%	4.52%
TPS		*BV-TG43*	*BV-Acuros*	*Difference*	*BV-TG43*	*BV-Acuros*	*Difference*
	1	99.52%	100.00%	0.48%	89.92%	100.00%	10.08%
	2	51.12%	51.34%	0.22%	59.99%	66.15%	6.16%
	3	31.48%	31.57%	0.09%	42.09%	46.25%	4.16%

All results were normalized to the air cavity trial for each plan. The dose difference between the water and air cavity is less than 2% for the symmetric plan, but nearly 13% for the asymmetric plan. In the symmetric plan, the dose difference is less than 1% when more than 2cm away from the applicator, while in the asymmetric plan, significant dose difference exist at 2 and 3cm away. Therefore, asymmetric plans experience a greater effect from changes in the cavity's contents than symmetric plans.

This is due to the greater average distance traveled in air by the photons in the asymmetric plan.

This data was compared to BrachyVision dose calculations for the SAVI device with an air cavity when using the TG-43 algorithm and Acuros. TG-43, not taking into account the air cavity, produces dosimetry similar to the MCNP data for the water filled cavity. Acuros data is similar to MCNP data with the air cavity, accurately taking the heterogeneity into account. This is the case for both the symmetric and asymmetric plan.

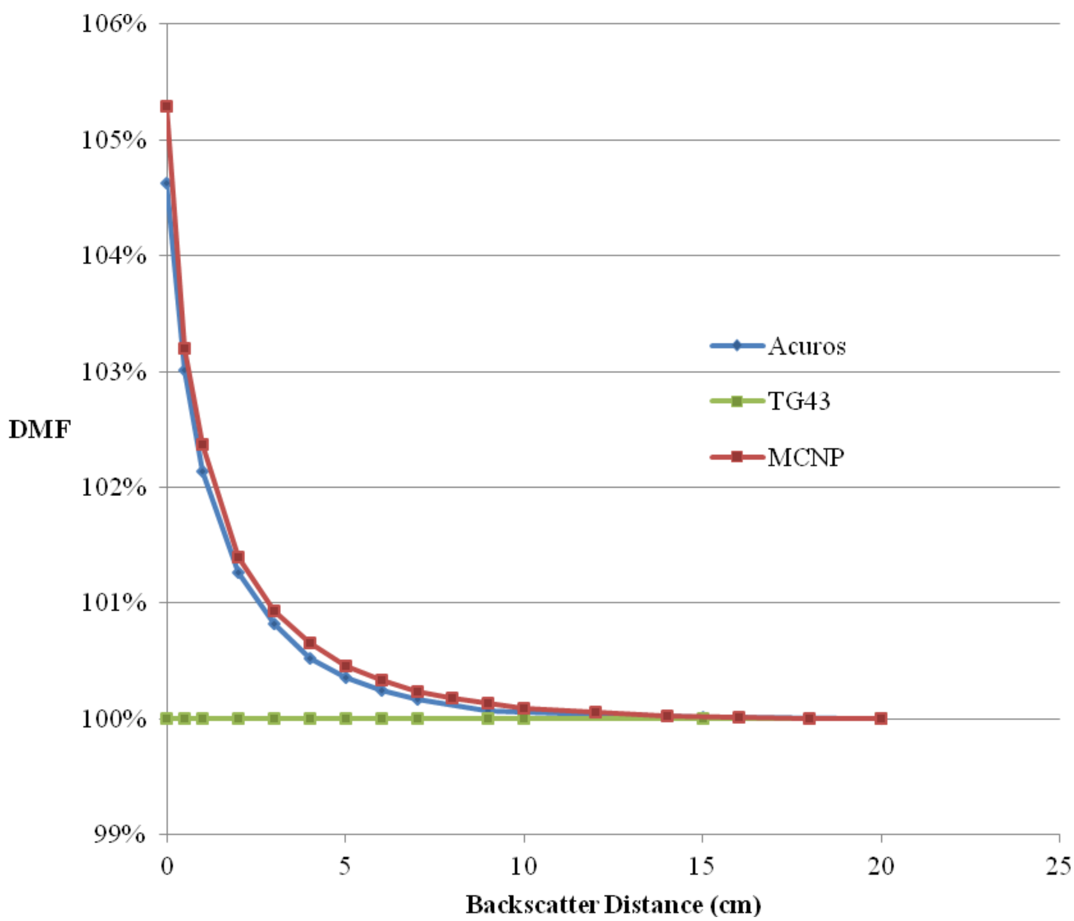

Figure 3-5: DMF's of MCNP base simulation, BrachyVision's TG-43 protocol algorithm (TG43), and BrachyVision's model-based dose calculation algorithm Acuros.

DMF's for the base Monte Carlo trial (cubic phantom, surrounded by water, water cavity, and symmetric plan) was compared to those found using BrachyVision. BrachyVision's TG-43 based algorithm and its model-based dose calculation algorithm were both used to measure the effects of backscatter. Results are presented in Figure 3-5. It is clear from the results the TG-43 does not account for differences in backscatter, as expected. The results from Acuros and MCNP are very similar, nearly 5% for both cases at 0cm backscatter, and similarly decreasing exponentially as the distance increases. The conclusion can be made from this that Acuros accurately accounts for differences in backscatter as suggested by Petrokokkinos *et al.* (Petrokokkinos, et al., 2011) and Zourari *et al* (Zourari, et al., 2010) (Zourari, et al., 2013).

Chapter 4

Conclusion

A model of the Strut-adjusted Volume Implant (SAVI) was created to be simulated in MCNP. Several trials were made based on this model. The base trial had symmetric dosimetry in a water cube with the SAVI's cavity filled with water. Four other trials used a spherical phantom rather than cubed, breast tissue rather than water inside the phantom, an air cavity rather than water, and final an asymmetric plan rather than a symmetric.

Comparing this model to previously simulated models and physical measurements, the model of the SAVI was validated.

The results of these trials supported the importance of heterogeneities being considered when performing brachytherapy dosimetry. Backscatter results showed that as much as 5% dose decrease in cases where the SAVI is close to a water-air interface. This was similar for each trial. Having an air cavity rather than a water cavity can change the relative dose 2% for a symmetric plan and up to 13% for an asymmetric plan. Considering a more realistic surrounding medium did not notably change the amount of dose delivered due to the close nature of water to that of average breast tissue.

When comparing MCNP results to TPS, it was clear that the TG-43 protocol did not account for the backscatter differences or heterogeneities tested. However, Acuros appeared to effectively account for differences in backscatter media and heterogeneities for both symmetric and asymmetric plans. Thus, it can be concluded that Acuros accounts for heterogeneities accurately for the SAVI applicator.

This thesis illustrates the importance of accounting for heterogeneities when considering SAVI dosimetry and brachytherapy dosimetry in general. Not accounting for differences in compositions can lead to inaccurate treatment plans and erroneous dose delivered to patients. It is recommended that based on the results presented in this thesis, clinics using this device should consider moving to the clinical usage of a model-based dose algorithm, such as BrachyVision-Acuros, following AAPM's TG-186 recommendations. This change will require adequate commissioning as outlined in TG-186 but will ensure more accurately delivery of brachytherapy treatments to future patients at the University of Toledo Medical Center.

References

American Cancer Society, 2012. *Cancer Facts & Figures.* [Online] Available at: www.seer.cancer.gov [Accessed 9 4 2013].

Arthur, M., 2008. A phase II trial of brachytherapy alone after lumpectomy for select breast cancer: tumor control and survival outcomes of RTOG 95-17. *Int. J. Radiation Oncology Biol. Phys.,* 2(72), pp. 467-473.

Bartelink, H., van Dam, F. & van Dongen, J., 1985. Psychological effects of breast conserving therapy in comparison with radical mastectomy. *Int. J. Radiat Oncol Biol Phys,* 2(11), pp. 381-5.

Beaulieu, L. et al., 2012. Report of the Task Group 186 on model-based dose calculation methods in brachytherapy beyond the TG-43 formalism: Current status and recommendations for clinical implementation. *Med Phys,* 39(10), pp. 6208-6236.

Benitez, P. et al., 2007. Five-year results: the initial clinical trial of MammoSite balloon brachytherapy for partial breast irradiation in early-stage breast cancer. *American Journal of Surgery,* Issue 194, pp. 456-462.

Brashears, J., Dragun, A. E. & Jenrette, J. M., 2009. Late chest wall toxicity after MammoSite breast brachytherapy. *Brachytherapy,* 1(8), pp. 19-25.

Brewster, A. et al., 2008. Residual Risk of Breast Cancer Recurrence 5 years After Adjuvant Therapy. *J Natl Can Inst,* Volume 100, pp. 1179-1183.

Brown, S. et al., 2012. Factors associated with chest wall toxicity after accelerated partial breast irradiation using high-dose-rate brachytherapy. *Int J Radiat Oncol Biol Phys,* 3(83), pp. 801-5.

Cazedca, M., Medich, D. & Munro, J., 2010. Effects of breast-air and breast-lung interfaces on the dose rate at the planning target volume of a MammoSite catheter for Yb-169 and Ir-192 HDR sources. *Med Phys,* 8(37), pp. 4038-45.

Clark, R., Whelan, T. & Levine, M., 1996. Randomized clincial trial of breast irradiation following lumpectomy and axillary dissection for node-negative breast cancer: an update. *J Natl Cancer Inst,* Issue 88, pp. 1659-1664.

Cuttino, L., Todor, D., Rosu, M. & Arthur, D. W., 2009. Skin and chest wall dose with multi-catheter and MammoSite breast brachytherapy: Implications for late toxicity. *Brachytherapy,* 2(8), pp. 223-6.

DeMarco, J., Kupelian, P., Santhanam, A. & Low, D., 2013. Shielding implications for secondary neutrons and photons produced within the patient during IMPT. *Med Phys,* Volume 40.

Dobelbower, R.R., Jr, Mitsuyuki Abe. Intraoperative Radiation Therapy. CRC Press, 1989.

Farr, J. et al., 2013. Fundmental radiological and geometric performance of two types of proton beam modulated discrete scanning systems. *Med Phys,* Volume 40.

Fisher, B., Anderson, S. & Bryant, J., 2002. Twenty-year follow-up of a randomized trial comparing total mastectomy, lumpectomy, and lumpectomy plus irradiation for the treatment of invasive breast cancer. *N Engl J Med,* Issue 347, pp. 1233-1241.

Formenti, S. C., Rosenstein, B., Skinner, K. A. & Jozsef, G., 2002. T1 Stage Breast Cancer: Adjuvant Hypofractionated Conformal Radiation Therapy to Tumor Bed in Selected Postmenopausal Breast Cancer Patients - Pilot Feasibility Study. *Radiology,* Issue 22, pp. 171-178.

Holli, K., Saaristo, R. & Isola, J., 2001. Lumpectomy with or without postoperative radiotherapy for breast cancer with favourable prognostic freatures: results of a randomized study. *Br J Cancer,* Issue 84, pp. 164-169.

Hyer, D., Sheybani, A., Jacobson, G. & Kim, Y., 2012. The dosimetric impact of heterogeneity corrections in high-dose-rate ^{192}Ir brachytherapy for cervical cancer: Investigation of both conventional Point-A and volume-optimized plans. *Brachytherapy,* 6(11), pp. 515-20.

Kassas, B., 2006. Dose Modification Factors for Ir-192 High-Dose-Rate Irradiation. *Journal of Applied Clinical Medical PHysics,* 7(3), pp. 28-34.

King, B. & Greer, P., 2013. A method for removing arm backscatter from EPID images. *Med Phys,* Volume 40.

Krishnaswamy, V., 1971. Calculation of the dose distribution about californium-252 needles in tissue. *Radiology,* Issue 98, pp. 155-160.

Lilijergren, G., Holmberg, L. & Bergh, J., 1999. 10-Year results after sector resection with or without postoperative radiotherapy for stage I breast cancer: a randomized trial. *J Clin Oncol,* Issue 17, pp. 2326-2333.

Meigooni, A., Meli, J. & Nath, R., 1992. Interseed effects on dose for 125I brachytherapy implants. *Med Phys,* 2(19), pp. 385-90.

Morris, A. et al., 1997. Breast-conserving therapy vs mastectomy in early-stage breast cancer: a meta-analysis of 10-year survival.. *Cancer J Sci Am,* 1(3), pp. 6-12.

Paixao, L. et al., 2012. Monte Carlo study of a new I-125 brachytherapy prototype seed with a ceramic radionuclide carrier and radiographic marker. *Journal of Applied Clinical Medical Physics,* 13(3).

Petrokokkinos, L. et al., 2011. Dosimetric accuracy of a deterministic radiation transport based Ir-192 brachytherapy treatment planning system. Part II: Monte Carlo and experimental verification of a multiple source dwell position plan employing a shielded applicator.. *Medical Physics,* pp. 1981-92.

Rivard, M. et al., 2004. Update of AAPM Task Group No. 43 Report: A revised AAPM protocol for brachytherapy dose calculations. *Med Phys,* Issue 31, pp. 633-674.

Scanderbeg, D. et al., 2009. Evaluation of three APBI techniques under NSABP B-39 guidelines. *J Appl Clin Med Phys,* 1(11), p. 3021.

Sherman, J., 2011. The Comparison of Dose Modification Factors for Two Multi-Lumen Brachtherapy Applicators used in Partial Breast Irradiation. *M.S. Thesis,* Volume University of Toledo.

Smith, T., Lee, D. & Turner, B., 2000. True recurrence vs. new primary ipsilateral breast tumor relapse: an analysis of clinical and pathologic difference and their implications in natural history, prognoses, and therapeutic management. *Int J Radiat Oncol Biol Phys,* Issue 48, pp. 1281-1289.

Thomadsen, B., Williamson, J. F., Rivard, M. J. & Meigooni, A. S., 2008. Anniversary paper: Past and current issues, and trends in brachytherapy physics. *Med Phys,* Issue 35, pp. 4708-4723.

Uniyal, S., Sharma, S. & Naithani, U., 2013. Dosimetric verification of a high dose rate brachytherapy treatment planning system in homogeneous and heterogeneous media. *Phys Med,* 2(29), pp. 171-7.

Vaidya, J. et al., 2001. Targeted intra-operative radiotherapy (Targit): An innovative method of treatment for early breast cancer. *Annals of Oncology,* Issue 12, pp. 1075-1080.

Veronesi, U., Cascinelli, N., Mariani, L. & Greco, M., 2002. Twenty-year follow-up of a randomized stdy comparing breast-conserving surgery with radical mastectomy for early breast cancer. *N Engl J Med,* Issue 347, pp. 1227-1232.

Vicini, F., 2007. Interim Cosmetic Results and Toxicity Using 3D Conformal External Beam Radiotherapy to Deliver Accelerated Partial Breast Irradiation in Patients with Early-Stage Breast Cancer Treated with Breast-Conserving Therapy. *International Journal of Radiation Oncology Biology Physics,* 69(4), pp. 1124-1130.

Vicini, F., Antonucci, J. V. & Wallace, M., 2007. Long-term efficacy and patterns of failure after accelerated partial breast irradiation: a molecular assay-based clonality evaulation. *Int J Radiat Oncol Biol Phys,* Issue 68, pp. 341-6.

Vicini, F. & Chen, P., 1997. Low-dose-rate brachytherapy as the sole radiation modality in the management of patients with early-stage breast cancer treated with breast-conserving therapy: prelimlinary results of a pilot trial. *Int J Radiat Oncol Biol Phys,* Issue 38, pp. 301-310.

Vicini, F., Kini, V. & Chen, P., 1999. Irradiation of the tumor bed alone after lumpectomy in selected patients with early-stage breast cancer treated with breast conserving therapy. *J Surg Oncol,* Issue 70, pp. 33-40.

Vicini, F., White, J. & Arthur, D., 2005. *A Randomized Phase III Study of Conventional Whole Breast Irradiation (WBI) Versus Partial Breast Irradiation (PBI) for Women with Stage 0, I, or II Breast Cancer,* s.l.: National Surgical Adjuvant Breast and Bowel Project (NSABP)/Radiation Therapy Oncology Group (RTOG).

Wazer, D., Arthur, D. & Vicini, F., 2006. *Accelerated Partial Breast Irradiation: techniques and clinical implementation.* Berlin: Springer.

Williams, E., 2012. Dose Modification Factor Analysis of Multi-Lumen Brachytherapy Applicator with Monte Carlo Simulation. *M.S. Thesis,* Volume University of Toledo.

Woodard, H. & White, D. R., 1986. The composition of body tissues. *British Journal of Radiology,* Volume 59, pp. 1209-1218.

Yashar, C., Blair, S., Wallace, A. & Scanderbeg, D., 2009. Initial clinical experience with the Strut-Adjusted Volume Implant brachytherapy applicator for accelerated partial breast irradiation. *Brachytherapy,* 4(8), pp. 367-72.

Zelefsky, M. & Whitemore, J. W. F., 1997. Long-term results of retropubic permanent I-125 implantation of the prostate for clinically localized prostatic cancer. *J Urol,* Issue 158, pp. 23-30.

Zourari, K. et al., 2010. Dosimetric accuracy of a deterministic radiation transport based Ir-192 brachytherapy treatment planning system. Part I: Single sources and bounded homogeneous geometries. *Medical Physics,* p. 649.

Zourari, K. et al., 2013. Dosimetric accuracy of a deterministic radiation transport based Ir-192 brachytherapy treatment planning system. Part III. Comparison to Monte Carlo simulation in voxelized anatomical computational models.. *Medical Physics,* p. 10.1118/1.4770275.

Appendix

A Code for MCNP model of SAVI

```
SAVI model:
c Geometries from "savi6" were adjusted by Craig Koontz in March 2013.
c ---------------------------------------------------------------------------|
c
c ****************************** Block 1: Cells *******************************
c
c ---------------------------------------------------------------------------|
c
c Center Lumen, #1
c
  101     2  -22.42 -101
  102     2  -22.42 -102
  103     2  -22.42 -103
  104     2  -22.42 -104
  105     2  -22.42 -105
  106     2  -22.42 -106
  107     2  -22.42 -107
  108     2  -22.42 -108
  109     2  -22.42 -109
  110     2  -22.42 -110
  111     2  -22.42 -111
  112     2  -22.42 -112
c
c Lumens are numbered clockwise
c Top Lumen, #2
c
  201     2  -22.42 -201
  202     2  -22.42 -202
  203     2  -22.42 -203
  204     2  -22.42 -204
  205     2  -22.42 -205
  206     2  -22.42 -206
  207     2  -22.42 -207
  208     2  -22.42 -208
  209     2  -22.42 -209
  210     2  -22.42 -210
  211     2  -22.42 -211
  212     2  -22.42 -212
  213     2  -22.42 -213
c
c   Lumen 3
c
  301     2  -22.42 -301
  302     2  -22.42 -302
  303     2  -22.42 -303
  304     2  -22.42 -304
  305     2  -22.42 -305
  306     2  -22.42 -306
  307     2  -22.42 -307
  308     2  -22.42 -308
  309     2  -22.42 -309
  310     2  -22.42 -310
  311     2  -22.42 -311
```

```
 312    2  -22.42 -312
 313    2  -22.42 -313
c
c   Lumen 4
c
 401    2  -22.42 -401
 402    2  -22.42 -402
 403    2  -22.42 -403
 404    2  -22.42 -404
 405    2  -22.42 -405
 406    2  -22.42 -406
 407    2  -22.42 -407
 408    2  -22.42 -408
 409    2  -22.42 -409
 410    2  -22.42 -410
 411    2  -22.42 -411
 412    2  -22.42 -412
 413    2  -22.42 -413
c
c   Lumen 5
c
 501    2  -22.42 -501
 502    2  -22.42 -502
 503    2  -22.42 -503
 504    2  -22.42 -504
 505    2  -22.42 -505
 506    2  -22.42 -506
 507    2  -22.42 -507
 508    2  -22.42 -508
 509    2  -22.42 -509
 510    2  -22.42 -510
 511    2  -22.42 -511
 512    2  -22.42 -512
 513    2  -22.42 -513
c
c   Lumen 6
c
 601    2  -22.42 -601
 602    2  -22.42 -602
 603    2  -22.42 -603
 604    2  -22.42 -604
 605    2  -22.42 -605
 606    2  -22.42 -606
 607    2  -22.42 -607
 608    2  -22.42 -608
 609    2  -22.42 -609
 610    2  -22.42 -610
 611    2  -22.42 -611
 612    2  -22.42 -612
 613    2  -22.42 -613
c
c Lumen 7
c
 701    2  -22.42 -701
 702    2  -22.42 -702
 703    2  -22.42 -703
 704    2  -22.42 -704
 705    2  -22.42 -705
 706    2  -22.42 -706
 707    2  -22.42 -707
 708    2  -22.42 -708
 709    2  -22.42 -709
 710    2  -22.42 -710
 711    2  -22.42 -711
 712    2  -22.42 -712
 713    2  -22.42 -713
c
c Lumen 8
c
 801    2  -22.42 -801
```

```
  802     2  -22.42 -802
  803     2  -22.42 -803
  804     2  -22.42 -804
  805     2  -22.42 -805
  806     2  -22.42 -806
  807     2  -22.42 -807
  808     2  -22.42 -808
  809     2  -22.42 -809
  810     2  -22.42 -810
  811     2  -22.42 -811
  812     2  -22.42 -812
  813     2  -22.42 -813
c
c Lumen 9
c
  901     2  -22.42 -901
  902     2  -22.42 -902
  903     2  -22.42 -903
  904     2  -22.42 -904
  905     2  -22.42 -905
  906     2  -22.42 -906
  907     2  -22.42 -907
  908     2  -22.42 -908
  909     2  -22.42 -909
  910     2  -22.42 -910
  911     2  -22.42 -911
  912     2  -22.42 -912
  913     2  -22.42 -913
c
c Water, both outside and inside lumen cavity
c
950 1 -1 -950 101 102 103 104 105 106 107 108 109 110 111 112 &
 201 202 203 204 205 206 207 208 209 210 211 212 213 &
 301 302 303 304 305 306 307 308 309 310 311 312 313 &
 401 402 403 404 405 406 407 408 409 410 411 412 413 &
 501 502 503 504 505 506 507 508 509 510 511 512 513 &
 601 602 603 604 605 606 607 608 609 610 611 612 613 &
 701 702 703 704 705 706 707 708 709 710 711 712 713 &
 801 802 803 804 805 806 807 808 809 810 811 812 813 &
 901 902 903 904 905 906 907 908 909 910 911 912 913 &
 960 961 962 963 964 965 966
c
c Air surrounding water
c
951 3 -0.001225 -951 950 960 961 962 963 964 965 966
c
c Tallies within water, made of water
c
960 1 -1 -960
961 1 -1 -961
962 1 -1 -962
963 1 -1 -963
964 1 -1 -964
965 1 -1 -965
966 1 -1 -966
c
c Graveyard
c
999 0 951

c ------------------------------------------------------------------------------|
c
c ****************************** Block 2: Surface Cards ************************
c
c ------------------------------------------------------------------------------|
c
c Lumen 1, Central Lumen
c
 101 rcc -3.0000 0.0000 0.0000 0.5000 0.0000 0.0000 0.0170
 102 rcc -2.5000 0.0000 0.0000 0.5000 0.0000 0.0000 0.0170
```

```
 103 rcc -2.0000 0.0000 0.0000 0.5000 0.0000 0.0000 0.0170
 104 rcc -1.5000 0.0000 0.0000 0.5000 0.0000 0.0000 0.0170
 105 rcc -1.0000 0.0000 0.0000 0.5000 0.0000 0.0000 0.0170
 106 rcc -0.5000 0.0000 0.0000 0.5000 0.0000 0.0000 0.0170
 107 rcc 0.0000 0.0000 0.0000 0.5000 0.0000 0.0000 0.0170
 108 rcc 0.5000 0.0000 0.0000 0.5000 0.0000 0.0000 0.0170
 109 rcc 1.0000 0.0000 0.0000 0.5000 0.0000 0.0000 0.0170
 110 rcc 1.5000 0.0000 0.0000 0.5000 0.0000 0.0000 0.0170
 111 rcc 2.0000 0.0000 0.0000 0.5000 0.0000 0.0000 0.0170
 112 rcc 2.5000 0.0000 0.0000 0.5000 0.0000 0.0000 0.0170
c
c Lumen 2
c
201 rcc -3 0 0.31 0.4411 0 0.2354 0.017
202 rcc -2.55 0 0.555 0.4239 0 0.2652 0.017
203 rcc -2.11 0 0.8303 0.4106 0 0.2853 0.017
204 rcc -1.6806 0 1.1314 0.3819 0 0.3227 0.017
205 rcc -1.28 0 1.47 0.4552 0 0.2068 0.017
206 rcc -0.77 0 1.7 0.4903 0 0.0981 0.017
207 rcc -0.25 0 1.8 0.5 0 0 0.017
208 rcc 0.77 0 1.7 -0.4903 0 0.0981 0.017
209 rcc 1.28 0 1.47 -0.4552 0 0.2068 0.017
210 rcc 1.6806 0 1.1314 -0.3819 0 0.3227 0.017
211 rcc 2.11 0 0.83 -0.4 0 0.3 0.017
212 rcc 2.55 0 0.555 -0.4239 0 0.2652 0.017
213 rcc 3 0 0.31 -0.4411 0 0.2354 0.017
c
c Lumen 3
c
  301      rcc -3 0.219 0.219 0.4676 0.1251 0.1251 0.017
  302      rcc -2.5296 0.3536 0.3536 0.3902 0.2211 0.2211 0.017
  303      rcc -2.1059 0.5936 0.5936 0.3937 0.2179 0.2179 0.017
  304      rcc -1.6944 0.821 0.821 0.4009 0.2113 0.2113 0.017
  305      rcc -1.2529 1.0481 1.0481 0.44558 0.1454 0.1454 0.017
  306      rcc -0.77 1.2021 1.2021 0.49 0.0704 0.0704 0.017
  307      rcc -0.25 1.273 1.273 0.5 0 0 0.017
  308      rcc 0.77 1.2021 1.2021 -0.49 0.0704 0.0704 0.017
  309      rcc 1.2529 1.0481 1.0481 -0.44558 0.1454 0.1454 0.017
  310      rcc 1.6944 0.821 0.821 -0.4009 0.2113 0.2113 0.017
  311      rcc 2.1059 0.5936 0.5936 -0.3937 0.2179 0.2179 0.017
  312      rcc 2.5296 0.3536 0.3536 -0.3902 0.2211 0.2211 0.017
  313      rcc 3 0.219 0.219 -0.4676 0.1251 0.1251 0.017
c
c Lumen 4
c
401 rcc -3 0.31 0 0.4411 0.2354 0 0.017
402 rcc -2.55 0.555 0 0.4239 0.2652 0 0.017
403 rcc -2.11 0.8303 0 0.4106 0.2853 0 0.017
404 rcc -1.6806 1.1314 0 0.3819 0.3227 0 0.017
405 rcc -1.28 1.47 0 0.4552 0.2068 0 0.017
406 rcc -0.77 1.7 0 0.4903 0.0981 0 0.017
407 rcc -0.25 1.8 0 0.5 0 0 0.017
408 rcc 0.77 1.7 0 -0.4903 0.0981 0 0.017
409 rcc 1.28 1.47 0 -0.4552 0.2068 0 0.017
410 rcc 1.6806 1.1314 0 -0.3819 0.3227 0 0.017
411 rcc 2.11 0.83 0 -0.4 0.3 0 0.017
412 rcc 2.55 0.555 0 -0.4239 0.2652 0 0.017
413 rcc 3 0.31 0 -0.4411 0.2354 0 0.017
c
c Lumen 5
c
  501      rcc -3 0.219 -0.219 0.4676 0.1251 -0.1251 0.017
  502      rcc -2.5296 0.3536 -0.3536 0.3902 0.2211 -0.2211 0.017
  503      rcc -2.1059 0.5936 -0.5936 0.3937 0.2179 -0.2179 0.017
  504      rcc -1.6944 0.821 -0.821 0.4009 0.2113 -0.2113 0.017
  505      rcc -1.2529 1.0481 -1.0481 0.44558 0.1454 -0.1454 0.017
  506      rcc -0.77 1.2021 -1.2021 0.49 0.0704 -0.0704 0.017
  507      rcc -0.25 1.273 -1.273 0.5 0 0 0.017
  508      rcc 0.77 1.2021 -1.2021 -0.49 0.0704 -0.0704 0.017
  509      rcc 1.2529 1.0481 -1.0481 -0.44558 0.1454 -0.1454 0.017
```

```
  510      rcc 1.6944 0.821 -0.821 -0.4009 0.2113 -0.2113 0.017
  511      rcc 2.1059 0.5936 -0.5936 -0.3937 0.2179 -0.2179 0.017
  512      rcc 2.5296 0.3536 -0.3536 -0.3902 0.2211 -0.2211 0.017
  513      rcc 3 0.219 -0.219 -0.4676 0.1251 -0.1251 0.017
c
c lumen 6
c
601 rcc -3 0 -0.31 0.4411 0 -0.2354 0.017
602 rcc -2.55 0 -0.555 0.4239 0 -0.2652 0.017
603 rcc -2.11 0 -0.8303 0.4106 0 -0.2853 0.017
604 rcc -1.6806 0 -1.1314 0.3819 0 -0.3227 0.017
605 rcc -1.28 0 -1.47 0.4552 0 -0.2068 0.017
606 rcc -0.77 0 -1.7 0.4903 0 -0.0981 0.017
607 rcc -0.25 0 -1.8 0.5 0 0 0.017
608 rcc 0.77 0 -1.7 -0.4903 0 -0.0981 0.017
609 rcc 1.28 0 -1.47 -0.4552 0 -0.2068 0.017
610 rcc 1.6806 0 -1.1314 -0.3819 0 -0.3227 0.017
611 rcc 2.11 0 -0.83 -0.4 0 -0.3 0.017
612 rcc 2.55 0 -0.555 -0.4239 0 -0.2652 0.017
613 rcc 3 0 -0.31 -0.4411 0 -0.2354 0.017
c
c Lumen 7
c
  701      rcc -3 -0.219 -0.219 0.4676 -0.1251 -0.1251 0.017
  702      rcc -2.5296 -0.3536 -0.3536 0.3902 -0.2211 -0.2211 0.017
  703      rcc -2.1059 -0.5936 -0.5936 0.3937 -0.2179 -0.2179 0.017
  704      rcc -1.6944 -0.821 -0.821 0.4009 -0.2113 -0.2113 0.017
  705      rcc -1.2529 -1.0481 -1.0481 0.44558 -0.1454 -0.1454 0.017
  706      rcc -0.77 -1.2021 -1.2021 0.49 -0.0704 -0.0704 0.017
  707      rcc -0.25 -1.273 -1.273 0.5 0 0 0.017
  708      rcc 0.77 -1.2021 -1.2021 -0.49 -0.0704 -0.0704 0.017
  709      rcc 1.2529 -1.0481 -1.0481 -0.44558 -0.1454 -0.1454 0.017
  710      rcc 1.6944 -0.821 -0.821 -0.4009 -0.2113 -0.2113 0.017
  711      rcc 2.1059 -0.5936 -0.5936 -0.3937 -0.2179 -0.2179 0.017
  712      rcc 2.5296 -0.3536 -0.3536 -0.3902 -0.2211 -0.2211 0.017
  713      rcc 3 -0.219 -0.219 -0.4676 -0.1251 -0.1251 0.017
c
c Lumen 8
c
 801 rcc -3.0000 -0.3100 0.0000 0.4411 -0.2354 0.0000 0.0170
 802 rcc -2.5500 -0.5550 0.0000 0.4239 -0.2652 0.0000 0.0170
 803 rcc -2.1100 -0.8303 0.0000 0.4106 -0.2853 0.0000 0.0170
 804 rcc -1.6806 -1.1314 0.0000 0.3819 -0.3227 0.0000 0.0170
 805 rcc -1.2800 -1.4700 0.0000 0.4552 -0.2068 0.0000 0.0170
 806 rcc -0.7700 -1.7000 0.0000 0.4903 -0.0981 0.0000 0.0170
 807 rcc -0.2500 -1.8000 0.0000 0.5000 0.0000 0.0000 0.0170
 808 rcc 0.7700 -1.7000 0.0000 -0.4903 -0.0981 0.0000 0.0170
 809 rcc 1.2800 -1.4700 0.0000 -0.4552 -0.2068 0.0000 0.0170
 810 rcc 1.6806 -1.1314 0.0000 -0.3819 -0.3227 0.0000 0.0170
 811 rcc 2.1100 -0.8300 0.0000 -0.4000 -0.3000 0.0000 0.0170
 812 rcc 2.5500 -0.5550 0.0000 -0.4239 -0.2652 0.0000 0.0170
 813 rcc 3.0000 -0.3100 0.0000 -0.4411 -0.2354 0.0000 0.0170
c
c Lumen 9
c
  901      rcc -3 -0.219 0.219 0.4676 -0.1251 0.1251 0.017
  902      rcc -2.5296 -0.3536 0.3536 0.3902 -0.2211 0.2211 0.017
  903      rcc -2.1059 -0.5936 0.5936 0.3937 -0.2179 0.2179 0.017
  904      rcc -1.6944 -0.821 0.821 0.4009 -0.2113 0.2113 0.017
  905      rcc -1.2529 -1.0481 1.0481 0.44558 -0.1454 0.1454 0.017
  906      rcc -0.77 -1.2021 1.2021 0.49 -0.0704 0.0704 0.017
  907      rcc -0.25 -1.273 1.273 0.5 0 0 0.017
  908      rcc 0.77 -1.2021 1.2021 -0.49 -0.0704 0.0704 0.017
  909      rcc 1.2529 -1.0481 1.0481 -0.44558 -0.1454 0.1454 0.017
  910      rcc 1.6944 -0.821 0.821 -0.4009 -0.2113 0.2113 0.017
  911      rcc 2.1059 -0.5936 0.5936 -0.3937 -0.2179 0.2179 0.017
  912      rcc 2.5296 -0.3536 0.3536 -0.3902 -0.2211 0.2211 0.017
  913      rcc 3 -0.219 0.219 -0.4676 -0.1251 0.1251 0.017
c
c Water
```

```
c
950 BOX -22.8 -22.8 -22.8 45.6 0 0 0 45.6 0 0 0 45.6
c
c Air
c
951 BOX -50 -50 -50 100 0 0 0 100 0 0 0 100
c
c Tallies
c
960 SZ 2.8 0.17
961 SZ 3.8 0.17
962 SY 2.8 0.17
963 SZ -2.8 0.17
964 SX 4 0.17
965 SX -4 0.17
966 SZ 4.8 0.17

mode  p
c
c Materials
c
m1    1000.               2  $Water
      8000.               1
m2    77192.              1  $Ir-192 Source
m3    7000.            -0.79  $Air
      18000.          -0.01
      8000.           -0.2
c ---------------------------------------------------------------------------
c Importance is for photons, then the importance is 1 for each cell,
c repeating N number of times (N = number before r, r for repeat) then
c 0 importance for final cell, the graveyard.
c ---------------------------------------------------------------------------
imp:p 1 124r 0
c ---------------------------------------------------------------------------
c
c ****************************** Block 3: Data Cards ***********************
c Cylindrical source cells are created in the following block.  All cylinders
c are oriented in the X-direction.  With the surfaces defined on different
c axes, the efficiency of these cards is not optimal, but greater the 1%.
c However, effenciency limit is set lower, 0.05%.
c ---------------------------------------------------------------------------
sdef CEL=d1 POS=FCEL d2 RAD=FCEL d119 EXT=FCEL d236 ERG=FCEL d353 AXS=1 0 0 &
   EFF=0.0005
     par 2
c
si1 L 101 102 103 104 105 106 107 108 109 110 111 112 &
  201 202 203 204 205 206 207 208 209 210 211 212 213 &
  301 302 303 304 305 306 307 308 309 310 311 312 313 &
  401 402 403 404 405 406 407 408 409 410 411 412 413 &
  501 502 503 504 505 506 507 508 509 510 511 512 513 &
  601 602 603 604 605 606 607 608 609 610 611 612 613 &
  701 702 703 704 705 706 707 708 709 710 711 712 713 &
  801 802 803 804 805 806 807 808 809 810 811 812 813 &
  901 902 903 904 905 906 907 908 909 910 911 912 913
c
c Normalized time for the sources in the order above 116
c
sp1 0.02025 0.0052 0.00225 0.00125 0.00215 0.0021 &
0.0021 0.00215 0.00125 0.00225 0.0052 0.02025 &
0.0096 0.0022 0.0052 0.00735 0.0111 0.0141 0.0176 &
0.0141 0.0111 0.00735 0.0052 0.0022 0.0096 &
0.0096 0.0022 0.0052 0.00735 0.0111 0.0141 0.0176 &
0.0141 0.0111 0.00735 0.0052 0.0022 0.0096 &
0.0096 0.0022 0.0052 0.00735 0.0111 0.0141 0.0176 &
0.0141 0.0111 0.00735 0.0052 0.0022 0.0096 &
0.0096 0.0022 0.0052 0.00735 0.0111 0.0141 0.0176 &
0.0141 0.0111 0.00735 0.0052 0.0022 0.0096 &
0.0096 0.0022 0.0052 0.00735 0.0111 0.0141 0.0176 &
0.0141 0.0111 0.00735 0.0052 0.0022 0.0096 &
0.0096 0.0022 0.0052 0.00735 0.0111 0.0141 0.0176 &
```

```
0.0141 0.0111 0.00735 0.0052 0.0022 0.0096 &
0.0096 0.0022 0.0052 0.00735 0.0111 0.0141 0.0176 &
0.0141 0.0111 0.00735 0.0052 0.0022 0.0096 &
0.0096 0.0022 0.0052 0.00735 0.0111 0.0141 0.0176 &
0.0141 0.0111 0.00735 0.0052 0.0022 0.0096
c
c  set POS for each source
c
ds2 S 003 004 005 006 007 008 009 010 011 012 &
013 014 015 016 017 018 019 020 021 022 &
023 024 025 026 027 028 029 030 031 032 &
033 034 035 036 037 038 039 040 041 042 &
043 044 045 046 047 048 049 050 051 052 &
053 054 055 056 057 058 059 060 061 062 &
063 064 065 066 067 068 069 070 071 072 &
073 074 075 076 077 078 079 080 081 082 &
083 084 085 086 087 088 089 090 091 092 &
093 094 095 096 097 098 099 100 101 102 &
103 104 105 106 107 108 109 110 111 112 &
113 114 115 116 117 118
c
c   Lumen 1
c
si003 L -2.7500 0.0000 0.0000
sp003 1.0000
si004 L -2.2500 0.0000 0.0000
sp004 1.0000
si005 L -1.7500 0.0000 0.0000
sp005 1.0000
si006 L -1.2500 0.0000 0.0000
sp006 1.0000
si007 L -0.7500 0.0000 0.0000
sp007 1.0000
si008 L -0.2500 0.0000 0.0000
sp008 1.0000
si009 L 0.2500 0.0000 0.0000
sp009 1.0000
si010 L 0.7500 0.0000 0.0000
sp010 1.0000
si011 L 1.2500 0.0000 0.0000
sp011 1.0000
si012 L 1.7500 0.0000 0.0000
sp012 1.0000
si013 L 2.2500 0.0000 0.0000
sp013 1.0000
si014 L 2.7500 0.0000 0.0000
sp014 1.0000
c
c   Lumen 2
c
si015 L -2.7795 0.0000 0.4277
sp015 1.0000
si016 L -2.3380 0.0000 0.6877
sp016 1.0000
si017 L -1.9047 0.0000 0.973
sp017 1.0000
si018 L -1.4897 0.0000 1.2928
sp018 1.0000
si019 L -1.0524 0.0000 1.5734
sp019 1.0000
si020 L -0.5249 0.0000 1.7490
sp020 1.0000
si021 L 0.0000 0.0000 1.8000
sp021 1.0000
si022 L 0.5249 0.0000 1.7490
sp022 1.0000
si023 L 1.0524 0.0000 1.5734
sp023 1.0000
si024 L 1.4897 0.0000 1.2928
sp024 1.0000
```

```
si025 L 1.9100 0.0000 0.9800
sp025 1.0000
si026 L 2.3380 0.0000 0.6877
sp026 1.0000
si027 L 2.7795 0.0000 0.4277
sp027 1.0000
c
c   Lumen 3
c
si028 L -2.7662 0.2816 0.2816
sp028 1
si029 L -2.3345 0.4641 0.4641
sp029 1
si030 L -1.9090 0.7026 0.7026
sp030 1
si031 L -1.4940 0.9266 0.9266
sp031 1
si032 L -1.0259 1.1222 1.1222
sp032 1
si033 L -0.5250 1.2373 1.2373
sp033 1
si034 L 0.0000 1.2730 1.2730
sp034 1
si035 L 0.5250 1.2373 1.2373
sp035 1
si036 L 1.0259 1.1222 1.1222
sp036 1
si037 L 1.4940 0.9266 0.9266
sp037 1
si038 L 1.9090 0.7026 0.7026
sp038 1
si039 L 2.3345 0.4641 0.4641
sp039 1
si040 L 2.7662 0.2816 0.2816
sp040 1
c
c   Lumen 4
c
si041 L -2.7795 0.4277 0.0000
sp041 1.0000
si042 L -2.3380 0.6877 0.0000
sp042 1.0000
si043 L -1.9047 0.9730 0.0000
sp043 1.0000
si044 L -1.4897 1.2928 0.0000
sp044 1.0000
si045 L -1.0524 1.5734 0.0000
sp045 1.0000
si046 L -0.5250 1.7490 0.0000
sp046 1.0000
si047 L 0.0000 1.8000 0.0000
sp047 1.0000
si048 L 0.5250 1.7490 0.0000
sp048 1.0000
si049 L 1.0524 1.5734 0.0000
sp049 1.0000
si050 L 1.4897 1.2928 0.0000
sp050 1.0000
si051 L 1.9100 0.9800 0.0000
sp051 1.0000
si052 L 2.3380 0.6877 0.0000
sp052 1.0000
si053 L 2.7795 0.4277 0.0000
sp053 1.0000
c
c   Lumen 5
c
si054 L -2.7662 0.2816 -0.2816
sp054 1
si055 L -2.3345 0.4641 -0.4641
```

sp055 1
si056 L -1.9090 0.7026 -0.7026
sp056 1
si057 L -1.4940 0.9266 -0.9266
sp057 1
si058 L -1.0259 1.1222 -1.1222
sp058 1
si059 L -0.5250 1.2373 -1.2373
sp059 1
si060 L 0.0000 1.2730 -1.2730
sp060 1
si061 L 0.5250 1.2373 -1.2373
sp061 1
si062 L 1.0259 1.1222 -1.1222
sp062 1
si063 L 1.4940 0.9266 -0.9266
sp063 1
si064 L 1.9090 0.7026 -0.7026
sp064 1
si065 L 2.3345 0.4641 -0.4641
sp065 1
si066 L 2.7662 0.2816 -0.2816
sp066 1
c
c Lumen 6
c
si067 L -2.7795 0.0000 -0.4277
sp067 1.0000
si068 L -2.3380 0.0000 -0.6877
sp068 1.0000
si069 L -1.9047 0.0000 -0.973
sp069 1.0000
si070 L -1.4897 0.0000 -1.2928
sp070 1.0000
si071 L -1.0524 0.0000 -1.5734
sp071 1.0000
si072 L -0.5250 0.0000 -1.7490
sp072 1.0000
si073 L 0.0000 0.0000 -1.8000
sp073 1.0000
si074 L 0.5250 0.0000 -1.7490
sp074 1.0000
si075 L 1.0524 0.0000 -1.5734
sp075 1.0000
si076 L 1.4897 0.0000 -1.2928
sp076 1.0000
si077 L 1.9000 0.0000 -0.9800
sp077 1.0000
si078 L 2.3380 0.0000 -0.6877
sp078 1.0000
si079 L 2.7795 0.0000 -0.4277
sp079 1.0000
c
c Lumen 7
c
si080 L -2.7662 -0.2816 -0.2816
sp080 1
si081 L -2.3345 -0.4641 -0.4641
sp081 1
si082 L -1.9090 -0.7026 -0.7026
sp082 1
si083 L -1.4940 -0.9266 -0.9266
sp083 1
si084 L -1.0259 -1.1222 -1.1222
sp084 1
si085 L -0.5250 -1.2373 -1.2373
sp085 1
si086 L 0.0000 -1.2730 -1.2730
sp086 1
si087 L 0.5250 -1.2373 -1.2373

```
sp087 1
si088 L 1.0259 -1.1222 -1.1222
sp088 1
si089 L 1.4940 -0.9266 -0.9266
sp089 1
si090 L 1.9090 -0.7026 -0.7026
sp090 1
si091 L 2.3345 -0.4641 -0.4641
sp091 1
si092 L 2.7662 -0.2816 -0.2816
sp092 1
c
c   Lumen 8
c
si093 L -2.7794 -0.4277 0.0000
sp093 1
si094 L -2.3381 -0.6876 0.0000
sp094 1
si095 L -1.9047 -0.9730 0.0000
sp095 1
si096 L -1.4897 -1.2928 0.0000
sp096 1
si097 L -1.0524 -1.5734 0.0000
sp097 1
si098 L -0.5249 -1.7490 0.0000
sp098 1
si099 L 0.0000 -1.8000 0.0000
sp099 1
si100 L 0.5249 -1.7490 0.0000
sp100 1
si101 L 1.0524 -1.5734 0.0000
sp101 1
si102 L 1.4897 -1.2928 0.0000
sp102 1
si103 L 1.9100 -0.9800 0.0000
sp103 1
si104 L 2.3381 -0.6876 0.0000
sp104 1
si105 L 2.7794 -0.4277 0.0000
sp105 1
c
c   Lumen 9
c
si106 L -2.7662 -0.2816 0.2816
sp106 1
si107 L -2.3345 -0.4641 0.4641
sp107 1
si108 L -1.9090 -0.7026 0.7026
sp108 1
si109 L -1.4940 -0.9266 0.9266
sp109 1
si110 L -1.0259 -1.1222 1.1222
sp110 1
si111 L -0.5250 -1.2373 1.2373
sp111 1
si112 L 0.0000 -1.2730 1.2730
sp112 1
si113 L 0.5250 -1.2373 1.2373
sp113 1
si114 L 1.0259 -1.1222 1.1222
sp114 1
si115 L 1.4940 -0.9266 0.9266
sp115 1
si116 L 1.9090 -0.7026 0.7026
sp116 1
si117 L 2.3345 -0.4641 0.4641
sp117 1
si118 L 2.7662 -0.2816 0.2816
sp118 1
c
```

```
c   set RAD for each source (must cover the entire source)
c
ds119 S 120 121 122 123 124 125 126 127 128 129 &
  130 131 132 133 134 135 136 137 138 139 &
  140 141 142 143 144 145 146 147 148 149 &
  150 151 152 153 154 155 156 157 158 159 &
  160 161 162 163 164 165 166 167 168 169 &
  170 171 172 173 174 175 176 177 178 179 &
  180 181 182 183 184 185 186 187 188 189 &
  190 191 192 193 194 195 196 197 198 199 &
  200 201 202 203 204 205 206 207 208 209 &
  210 211 212 213 214 215 216 217 218 219 &
  220 221 222 223 224 225 226 227 228 229 &
  230 231 232 233 234 235
c
c   Lumen 1
c
si120 0 0.017
sp120 -21 1
si121 0 0.017
sp121 -21 1
si122 0 0.017
sp122 -21 1
si123 0 0.017
sp123 -21 1
si124 0 0.017
sp124 -21 1
si125 0 0.017
sp125 -21 1
si126 0 0.017
sp126 -21 1
si127 0 0.017
sp127 -21 1
si128 0 0.017
sp128 -21 1
si129 0 0.017
sp129 -21 1
si130 0 0.017
sp130 -21 1
si131 0 0.017
sp131 -21 1
c
c   Lumen 2
c
si132 0 0.13465
sp132 -21 1
si133 0 0.14965
sp133 -21 1
si134 0 0.1597
sp134 -21 1
si135 0 0.1784
sp135 -21 1
si136 0 0.1204
sp136 -21 1
si137 0 0.066
sp137 -21 1
si138 0 0.017
sp138 -21 1
si139 0 0.066
sp139 -21 1
si140 0 0.1204
sp140 -21 1
si141 0 0.1784
sp141 -21 1
si142 0 0.167
sp142 -21 1
si143 0 0.14965
sp143 -21 1
si144 0 0.13465
sp144 -21 1
```

```
c
c   Lumen 3
c
si145 0 0.0966
sp145 -21 1
si146 0 0.1446
sp146 -21 1
si147 0 0.1430
sp147 -21 1
si148 0 0.1397
sp148 -21 1
si149 0 0.1067
sp149 -21 1
si150 0 0.0692
sp150 -21 1
si151 0 0.0340
sp151 -21 1
si152 0 0.0692
sp152 -21 1
si153 0 0.1067
sp153 -21 1
si154 0 0.1397
sp154 -21 1
si155 0 0.1430
sp155 -21 1
si156 0 0.1446
sp156 -21 1
si157 0 0.0966
sp157 -21 1
c
c   Lumen 4
c
si158 0 0.13465
sp158 -21 1
si159 0 0.14965
sp159 -21 1
si160 0 0.15965
sp160 -21 1
si161 0 0.1784
sp161 -21 1
si162 0 0.126
sp162 -21 1
si163 0 0.066
sp163 -21 1
si164 0 0.017
sp164 -21 1
si165 0 0.066
sp165 -21 1
si166 0 0.126
sp166 -21 1
si167 0 0.1784
sp167 -21 1
si168 0 0.167
sp168 -21 1
si169 0 0.14965
sp169 -21 1
si170 0 0.13465
sp170 -21 1
c
c   Lumen 5
c
si171 0 0.0966
sp171 -21 1
si172 0 0.1446
sp172 -21 1
si173 0 0.1430
sp173 -21 1
si174 0 0.1397
sp174 -21 1
si175 0 0.1067
```

```
sp175 -21 1
si176 0 0.0692
sp176 -21 1
si177 0 0.0340
sp177 -21 1
si178 0 0.0692
sp178 -21 1
si179 0 0.1067
sp179 -21 1
si180 0 0.1397
sp180 -21 1
si181 0 0.1430
sp181 -21 1
si182 0 0.1446
sp182 -21 1
si183 0 0.0966
sp183 -21 1
c
c   Lumen 6
c
si184 0 0.13465
sp184 -21 1
si185 0 0.14965
sp185 -21 1
si186 0 0.167
sp186 -21 1
si187 0 0.1784
sp187 -21 1
si188 0 0.126
sp188 -21 1
si189 0 0.066
sp189 -21 1
si190 0 0.017
sp190 -21 1
si191 0 0.066
sp191 -21 1
si192 0 0.126
sp192 -21 1
si193 0 0.1784
sp193 -21 1
si194 0 0.167
sp194 -21 1
si195 0 0.1496
sp195 -21 1
si196 0 0.13465
sp196 -21 1
c
c   Lumen 7
c
si197 0 0.0966
sp197 -21 1
si198 0 0.1446
sp198 -21 1
si199 0 0.1430
sp199 -21 1
si200 0 0.1397
sp200 -21 1
si201 0 0.1067
sp201 -21 1
si202 0 0.0692
sp202 -21 1
si203 0 0.0340
sp203 -21 1
si204 0 0.0692
sp204 -21 1
si205 0 0.1067
sp205 -21 1
si206 0 0.1397
sp206 -21 1
si207 0 0.1430
```

```
sp207 -21 1
si208 0 0.1446
sp208 -21 1
si209 0 0.0966
sp209 -21 1
c
c   Lumen 8
c
si210 0 0.1347
sp210 -21 1
si211 0 0.1496
sp211 -21 1
si212 0 0.1597
sp212 -21 1
si213 0 0.1784
sp213 -21 1
si214 0 0.1204
sp214 -21 1
si215 0 0.0661
sp215 -21 1
si216 0 0.0170
sp216 -21 1
si217 0 0.0661
sp217 -21 1
si218 0 0.1204
sp218 -21 1
si219 0 0.1784
sp219 -21 1
si220 0 0.1670
sp220 -21 1
si221 0 0.1496
sp221 -21 1
si222 0 0.1347
sp222 -21 1
c
c   Lumen 9
c
si223 0 0.0966
sp223 -21 1
si224 0 0.1446
sp224 -21 1
si225 0 0.1430
sp225 -21 1
si226 0 0.1397
sp226 -21 1
si227 0 0.1067
sp227 -21 1
si228 0 0.0692
sp228 -21 1
si229 0 0.0340
sp229 -21 1
si230 0 0.0692
sp230 -21 1
si231 0 0.1067
sp231 -21 1
si232 0 0.1397
sp232 -21 1
si233 0 0.1430
sp233 -21 1
si234 0 0.1446
sp234 -21 1
si235 0 0.0966
sp235 -21 1
c
c EXT for each source = length in the x-axis
c
ds236 S 237 238 239 240 241 242 243 244 245 246 247 248 249 250
      251 252 253 254 255 256 257 258 259 260 261 262 263 264
      265 266 267 268 269 270 271 272 273 274 275 276 277 278
      279 280 281 282 283 284 285 286 287 288 289 290 291 292
```

```
     293 294 295 296 297 298 299 300 301 302 303 304 305 306
     307 308 309 310 311 312 313 314 315 316 317 318 319 320
     321 322 323 324 325 326 327 328 329 330 331 332 333 334
     335 336 337 338 339 340 341 342 343 344 345 346 347 348
     349 350 351 352
c
c   Lumen 1
c
si237 -0.25 0.25
sp237 -21 0
si238 -0.25 0.25
sp238 -21 0
si239 -0.25 0.25
sp239 -21 0
si240 -0.25 0.25
sp240 -21 0
si241 -0.25 0.25
sp241 -21 0
si242 -0.25 0.25
sp242 -21 0
si243 -0.25 0.25
sp243 -21 0
si244 -0.25 0.25
sp244 -21 0
si245 -0.25 0.25
sp245 -21 0
si246 -0.25 0.25
sp246 -21 0
si247 -0.25 0.25
sp247 -21 0
si248 -0.25 0.25
sp248 -21 0
c
c   Lumen 2
c
si249 -0.2205 0.2205
sp249 -21 0
si250 -0.212 0.212
sp250 -21 0
si251 -0.2053 0.2053
sp251 -21 0
si252 -0.1910 0.1910
sp252 -21 0
si253 -0.23 0.23
sp253 -21 0
si254 -0.245 0.245
sp254 -21 0
si255 -0.25 0.25
sp255 -21 0
si256 -0.245 0.245
sp256 -21 0
si257 -0.23 0.23
sp257 -21 0
si258 -0.1910 0.1910
sp258 -21 0
si259 -0.2053 0.2053
sp259 -21 0
si260 -0.212 0.212
sp260 -21 0
si261 -0.2205 0.2205
sp261 -21 0
c
c   Lumen 3
c
si262 -0.2338 0.2338
sp262 -21 0
si263 -0.1951 0.1951
sp263 -21 0
si264 -0.1969 0.1969
sp264 -21 0
```

```
si265 -0.2004 0.2004
sp265 -21 0
si266 -0.2270 0.2270
sp266 -21 0
si267 -0.2450 0.2450
sp267 -21 0
si268 -0.2500 0.2500
sp268 -21 0
si269 -0.2450 0.2450
sp269 -21 0
si270 -0.2270 0.2270
sp270 -21 0
si271 -0.2004 0.2004
sp271 -21 0
si272 -0.1969 0.1969
sp272 -21 0
si273 -0.1951 0.1951
sp273 -21 0
si274 -0.2338 0.2338
sp274 -21 0
c
c   Lumen 4
c
si275 -0.2205 0.2205
sp275 -21 0
si276 -0.212 0.212
sp276 -21 0
si277 -0.2053 0.2053
sp277 -21 0
si278 -0.1910 0.1910
sp278 -21 0
si279 -0.24 0.24
sp279 -21 0
si280 -0.245 0.245
sp280 -21 0
si281 -0.25 0.25
sp281 -21 0
si282 -0.245 0.245
sp282 -21 0
si283 -0.24 0.24
sp283 -21 0
si284 -0.1910 0.1910
sp284 -21 0
si285 -0.2053 0.2053
sp285 -21 0
si286 -0.212 0.212
sp286 -21 0
si287 -0.2205 0.2205
sp287 -21 0
c
c   Lumen 5
c
si288 -0.2338 0.2338
sp288 -21 0
si289 -0.1951 0.1951
sp289 -21 0
si290 -0.1969 0.1969
sp290 -21 0
si291 -0.2004 0.2004
sp291 -21 0
si292 -0.2270 0.2270
sp292 -21 0
si293 -0.2450 0.2450
sp293 -21 0
si294 -0.2500 0.2500
sp294 -21 0
si295 -0.2450 0.2450
sp295 -21 0
si296 -0.2270 0.2270
sp296 -21 0
```

```
si297 -0.2004 0.2004
sp297 -21 0
si298 -0.1969 0.1969
sp298 -21 0
si299 -0.1951 0.1951
sp299 -21 0
si300 -0.2338 0.2338
sp300 -21 0
c
c   Lumen 6
c
si301 -0.2205 0.2205
sp301 -21 0
si302 -0.212 0.212
sp302 -21 0
si303 -0.2053 0.2053
sp303 -21 0
si304 -0.1910 0.1910
sp304 -21 0
si305 -0.24 0.24
sp305 -21 0
si306 -0.245 0.245
sp306 -21 0
si307 -0.25 0.25
sp307 -21 0
si308 -0.245 0.245
sp308 -21 0
si309 -0.24 0.24
sp309 -21 0
si310 -0.1910 0.1910
sp310 -21 0
si311 -0.2 0.2
sp311 -21 0
si312 -0.212 0.212
sp312 -21 0
si313 -0.2205 0.2205
sp313 -21 0
c
c   Lumen 7
c
si314 -0.2338 0.2338
sp314 -21 0
si315 -0.1951 0.1951
sp315 -21 0
si316 -0.1969 0.1969
sp316 -21 0
si317 -0.2004 0.2004
sp317 -21 0
si318 -0.2270 0.2270
sp318 -21 0
si319 -0.2450 0.2450
sp319 -21 0
si320 -0.2500 0.2500
sp320 -21 0
si321 -0.2450 0.2450
sp321 -21 0
si322 -0.2270 0.2270
sp322 -21 0
si323 -0.2004 0.2004
sp323 -21 0
si324 -0.1969 0.1969
sp324 -21 0
si325 -0.1951 0.1951
sp325 -21 0
si326 -0.2338 0.2338
sp326 -21 0
c
c   Lumen 8
c
si327 -0.220557777 0.2206
```

```
sp327 -21 0
si328 -0.211940569 0.2119
sp328 -21 0
si329 -0.2053 0.2053
sp329 -21 0
si330 -0.1910 0.1910
sp330 -21 0
si331 -0.24 0.24
sp331 -21 0
si332 -0.245141322 0.2451
sp332 -21 0
si333 -0.25 0.2500
sp333 -21 0
si334 -0.245141322 0.2451
sp334 -21 0
si335 -0.227612164 0.2276
sp335 -21 0
si336 -0.1910 0.1910
sp336 -21 0
si337 -0.2 0.2000
sp337 -21 0
si338 -0.212 0.212
sp338 -21 0
si339 -0.220557777 0.2206
sp339 -21 0
c
c   Lumen 9
c
si340 -0.2338 0.2338
sp340 -21 0
si341 -0.1951 0.1951
sp341 -21 0
si342 -0.1969 0.1969
sp342 -21 0
si343 -0.2004 0.2004
sp343 -21 0
si344 -0.2270 0.2270
sp344 -21 0
si345 -0.2450 0.2450
sp345 -21 0
si346 -0.2500 0.2500
sp346 -21 0
si347 -0.2450 0.2450
sp347 -21 0
si348 -0.2270 0.2270
sp348 -21 0
si349 -0.2004 0.2004
sp349 -21 0
si350 -0.1969 0.1969
sp350 -21 0
si351 -0.1951 0.1951
sp351 -21 0
si352 -0.2338 0.2338
sp352 -21 0
c
c  Source specification
c
ds353 S 354 355 356 357 358 359 360 361 362 363 364 365 366 367
      368 369 370 371 372 373 374 375 376 377 378 379 380 381
      382 383 384 385 386 387 388 389 390 391 392 393 394 395
      396 397 398 399 400 401 402 403 404 405 406 407 408 409
      410 411 412 413 414 415 416 417 418 419 420 421 422 423
      424 425 426 427 428 429 430 431 432 433 434 435 436 437
      438 439 440 441 442 443 444 445 446 447 448 449 450 451
      452 453 454 455 456 457 458 459 460 461 462 463 464 465
      466 467 468 469
c
c              add source values for each  cell
si354   L 0.2960 0.3085 0.3166 0.4681 0.5886 0.6044 0.6125
sp354     0.287 0.297 0.830 0.478 0.045 0.081 0.053
```

```
c
si355   L 0.2960 0.3085 0.3166 0.4681 0.5886 0.6044 0.6125
sp355     0.287 0.297 0.830 0.478 0.045 0.081 0.053
c
si356   L 0.2960 0.3085 0.3166 0.4681 0.5886 0.6044 0.6125
sp356     0.287 0.297 0.830 0.478 0.045 0.081 0.053
c
si357   L 0.2960 0.3085 0.3166 0.4681 0.5886 0.6044 0.6125
sp357     0.287 0.297 0.830 0.478 0.045 0.081 0.053
c
si358   L 0.2960 0.3085 0.3166 0.4681 0.5886 0.6044 0.6125
sp358     0.287 0.297 0.830 0.478 0.045 0.081 0.053
c
si359   L 0.2960 0.3085 0.3166 0.4681 0.5886 0.6044 0.6125
sp359     0.287 0.297 0.830 0.478 0.045 0.081 0.053
c
si360   L 0.2960 0.3085 0.3166 0.4681 0.5886 0.6044 0.6125
sp360     0.287 0.297 0.830 0.478 0.045 0.081 0.053
c
si361   L 0.2960 0.3085 0.3166 0.4681 0.5886 0.6044 0.6125
sp361     0.287 0.297 0.830 0.478 0.045 0.081 0.053
c
si362   L 0.2960 0.3085 0.3166 0.4681 0.5886 0.6044 0.6125
sp362     0.287 0.297 0.830 0.478 0.045 0.081 0.053
c
si363   L 0.2960 0.3085 0.3166 0.4681 0.5886 0.6044 0.6125
sp363     0.287 0.297 0.830 0.478 0.045 0.081 0.053
c
si364   L 0.2960 0.3085 0.3166 0.4681 0.5886 0.6044 0.6125
sp364     0.287 0.297 0.830 0.478 0.045 0.081 0.053
c
si365   L 0.2960 0.3085 0.3166 0.4681 0.5886 0.6044 0.6125
sp365     0.287 0.297 0.830 0.478 0.045 0.081 0.053
c
si366   L 0.2960 0.3085 0.3166 0.4681 0.5886 0.6044 0.6125
sp366     0.287 0.297 0.830 0.478 0.045 0.081 0.053
c
si367   L 0.2960 0.3085 0.3166 0.4681 0.5886 0.6044 0.6125
sp367     0.287 0.297 0.830 0.478 0.045 0.081 0.053
c
si368   L 0.2960 0.3085 0.3166 0.4681 0.5886 0.6044 0.6125
sp368     0.287 0.297 0.830 0.478 0.045 0.081 0.053
c
si369   L 0.2960 0.3085 0.3166 0.4681 0.5886 0.6044 0.6125
sp369     0.287 0.297 0.830 0.478 0.045 0.081 0.053
c
si370   L 0.2960 0.3085 0.3166 0.4681 0.5886 0.6044 0.6125
sp370     0.287 0.297 0.830 0.478 0.045 0.081 0.053
c
si371   L 0.2960 0.3085 0.3166 0.4681 0.5886 0.6044 0.6125
sp371     0.287 0.297 0.830 0.478 0.045 0.081 0.053
c
si372   L 0.2960 0.3085 0.3166 0.4681 0.5886 0.6044 0.6125
sp372     0.287 0.297 0.830 0.478 0.045 0.081 0.053
c
si373   L 0.2960 0.3085 0.3166 0.4681 0.5886 0.6044 0.6125
sp373     0.287 0.297 0.830 0.478 0.045 0.081 0.053
c
si374   L 0.2960 0.3085 0.3166 0.4681 0.5886 0.6044 0.6125
sp374     0.287 0.297 0.830 0.478 0.045 0.081 0.053
c
si375   L 0.2960 0.3085 0.3166 0.4681 0.5886 0.6044 0.6125
sp375     0.287 0.297 0.830 0.478 0.045 0.081 0.053
c
si376   L 0.2960 0.3085 0.3166 0.4681 0.5886 0.6044 0.6125
sp376     0.287 0.297 0.830 0.478 0.045 0.081 0.053
c
si377   L 0.2960 0.3085 0.3166 0.4681 0.5886 0.6044 0.6125
sp377     0.287 0.297 0.830 0.478 0.045 0.081 0.053
c
```

```
si378   L 0.2960 0.3085 0.3166 0.4681 0.5886 0.6044 0.6125
sp378     0.287 0.297 0.830 0.478 0.045 0.081 0.053
c
si379   L 0.2960 0.3085 0.3166 0.4681 0.5886 0.6044 0.6125
sp379   0.287 0.297 0.830 0.478 0.045 0.081 0.053
c
si380   L 0.2960 0.3085 0.3166 0.4681 0.5886 0.6044 0.6125
sp380     0.287 0.297 0.830 0.478 0.045 0.081 0.053
c
si381   L 0.2960 0.3085 0.3166 0.4681 0.5886 0.6044 0.6125
sp381     0.287 0.297 0.830 0.478 0.045 0.081 0.053
c
si382   L 0.2960 0.3085 0.3166 0.4681 0.5886 0.6044 0.6125
sp382     0.287 0.297 0.830 0.478 0.045 0.081 0.053
c
si383   L 0.2960 0.3085 0.3166 0.4681 0.5886 0.6044 0.6125
sp383     0.287 0.297 0.830 0.478 0.045 0.081 0.053
c
si384   L 0.2960 0.3085 0.3166 0.4681 0.5886 0.6044 0.6125
sp384     0.287 0.297 0.830 0.478 0.045 0.081 0.053
c
si385   L 0.2960 0.3085 0.3166 0.4681 0.5886 0.6044 0.6125
sp385     0.287 0.297 0.830 0.478 0.045 0.081 0.053
c
si386   L 0.2960 0.3085 0.3166 0.4681 0.5886 0.6044 0.6125
sp386     0.287 0.297 0.830 0.478 0.045 0.081 0.053
c
si387   L 0.2960 0.3085 0.3166 0.4681 0.5886 0.6044 0.6125
sp387     0.287 0.297 0.830 0.478 0.045 0.081 0.053
c
si388   L 0.2960 0.3085 0.3166 0.4681 0.5886 0.6044 0.6125
sp388     0.287 0.297 0.830 0.478 0.045 0.081 0.053
c
si389   L 0.2960 0.3085 0.3166 0.4681 0.5886 0.6044 0.6125
sp389     0.287 0.297 0.830 0.478 0.045 0.081 0.053
c
si390   L 0.2960 0.3085 0.3166 0.4681 0.5886 0.6044 0.6125
sp390     0.287 0.297 0.830 0.478 0.045 0.081 0.053
c
si391   L 0.2960 0.3085 0.3166 0.4681 0.5886 0.6044 0.6125
sp391     0.287 0.297 0.830 0.478 0.045 0.081 0.053
c
si392   L 0.2960 0.3085 0.3166 0.4681 0.5886 0.6044 0.6125
sp392    0.287 0.297 0.830 0.478 0.045 0.081 0.053
c
si393  L 0.2960 0.3085 0.3166 0.4681 0.5886 0.6044 0.6125
sp393  0.287 0.297 0.830 0.478 0.045 0.081 0.053
c
si394  L 0.2960 0.3085 0.3166 0.4681 0.5886 0.6044 0.6125
sp394  0.287 0.297 0.830 0.478 0.045 0.081 0.053
c
si395  L 0.2960 0.3085 0.3166 0.4681 0.5886 0.6044 0.6125
sp395  0.287 0.297 0.830 0.478 0.045 0.081 0.053
c
si396  L 0.2960 0.3085 0.3166 0.4681 0.5886 0.6044 0.6125
sp396  0.287 0.297 0.830 0.478 0.045 0.081 0.053
c
si397  L 0.2960 0.3085 0.3166 0.4681 0.5886 0.6044 0.6125
sp397  0.287 0.297 0.830 0.478 0.045 0.081 0.053
c
si398  L 0.2960 0.3085 0.3166 0.4681 0.5886 0.6044 0.6125
sp398  0.287 0.297 0.830 0.478 0.045 0.081 0.053
c
si399  L 0.2960 0.3085 0.3166 0.4681 0.5886 0.6044 0.6125
sp399  0.287 0.297 0.830 0.478 0.045 0.081 0.053
c
si400  L 0.2960 0.3085 0.3166 0.4681 0.5886 0.6044 0.6125
sp400     0.287 0.297 0.830 0.478 0.045 0.081 0.053
c
si401  L 0.2960 0.3085 0.3166 0.4681 0.5886 0.6044 0.6125
```

```
sp401     0.287 0.297 0.830 0.478 0.045 0.081 0.053
c
si402  L 0.2960 0.3085 0.3166 0.4681 0.5886 0.6044 0.6125
sp402  0.287 0.297 0.830 0.478 0.045 0.081 0.053
c
si403  L 0.2960 0.3085 0.3166 0.4681 0.5886 0.6044 0.6125
sp403  0.287 0.297 0.830 0.478 0.045 0.081 0.053
c
si404  L 0.2960 0.3085 0.3166 0.4681 0.5886 0.6044 0.6125
sp404  0.287 0.297 0.830 0.478 0.045 0.081 0.053
c
si405  L 0.2960 0.3085 0.3166 0.4681 0.5886 0.6044 0.6125
sp405  0.287 0.297 0.830 0.478 0.045 0.081 0.053
c
si406  L 0.2960 0.3085 0.3166 0.4681 0.5886 0.6044 0.6125
sp406  0.287 0.297 0.830 0.478 0.045 0.081 0.053
c
si407  L 0.2960 0.3085 0.3166 0.4681 0.5886 0.6044 0.6125
sp407  0.287 0.297 0.830 0.478 0.045 0.081 0.053
c
si408  L 0.2960 0.3085 0.3166 0.4681 0.5886 0.6044 0.6125
sp408  0.287 0.297 0.830 0.478 0.045 0.081 0.053
c
si409  L 0.2960 0.3085 0.3166 0.4681 0.5886 0.6044 0.6125
sp409  0.287 0.297 0.830 0.478 0.045 0.081 0.053
c
si410  L 0.2960 0.3085 0.3166 0.4681 0.5886 0.6044 0.6125
sp410  0.287 0.297 0.830 0.478 0.045 0.081 0.053
c
si411  L 0.2960 0.3085 0.3166 0.4681 0.5886 0.6044 0.6125
sp411  0.287 0.297 0.830 0.478 0.045 0.081 0.053
c
si412  L 0.2960 0.3085 0.3166 0.4681 0.5886 0.6044 0.6125
sp412  0.287 0.297 0.830 0.478 0.045 0.081 0.053
c
si413  L 0.2960 0.3085 0.3166 0.4681 0.5886 0.6044 0.6125
sp413  0.287 0.297 0.830 0.478 0.045 0.081 0.053
c
si414  L 0.2960 0.3085 0.3166 0.4681 0.5886 0.6044 0.6125
sp414  0.287 0.297 0.830 0.478 0.045 0.081 0.053
c
si415  L 0.2960 0.3085 0.3166 0.4681 0.5886 0.6044 0.6125
sp415  0.287 0.297 0.830 0.478 0.045 0.081 0.053
c
si416  L 0.2960 0.3085 0.3166 0.4681 0.5886 0.6044 0.6125
sp416  0.287 0.297 0.830 0.478 0.045 0.081 0.053
c
si417  L 0.2960 0.3085 0.3166 0.4681 0.5886 0.6044 0.6125
sp417  0.287 0.297 0.830 0.478 0.045 0.081 0.053
c
si418  L 0.2960 0.3085 0.3166 0.4681 0.5886 0.6044 0.6125
sp418  0.287 0.297 0.830 0.478 0.045 0.081 0.053
c
si419  L 0.2960 0.3085 0.3166 0.4681 0.5886 0.6044 0.6125
sp419  0.287 0.297 0.830 0.478 0.045 0.081 0.053
c
si420  L 0.2960 0.3085 0.3166 0.4681 0.5886 0.6044 0.6125
sp420  0.287 0.297 0.830 0.478 0.045 0.081 0.053
c
si421  L 0.2960 0.3085 0.3166 0.4681 0.5886 0.6044 0.6125
sp421  0.287 0.297 0.830 0.478 0.045 0.081 0.053
c
si422  L 0.2960 0.3085 0.3166 0.4681 0.5886 0.6044 0.6125
sp422  0.287 0.297 0.830 0.478 0.045 0.081 0.053
c
si423  L 0.2960 0.3085 0.3166 0.4681 0.5886 0.6044 0.6125
sp423  0.287 0.297 0.830 0.478 0.045 0.081 0.053
c
si424  L 0.2960 0.3085 0.3166 0.4681 0.5886 0.6044 0.6125
sp424  0.287 0.297 0.830 0.478 0.045 0.081 0.053
```

```
c
si425  L 0.2960 0.3085 0.3166 0.4681 0.5886 0.6044 0.6125
sp425  0.287 0.297 0.830 0.478 0.045 0.081 0.053
c
si426  L 0.2960 0.3085 0.3166 0.4681 0.5886 0.6044 0.6125
sp426  0.287 0.297 0.830 0.478 0.045 0.081 0.053
c
si427  L 0.2960 0.3085 0.3166 0.4681 0.5886 0.6044 0.6125
sp427  0.287 0.297 0.830 0.478 0.045 0.081 0.053
c
si428  L 0.2960 0.3085 0.3166 0.4681 0.5886 0.6044 0.6125
sp428  0.287 0.297 0.830 0.478 0.045 0.081 0.053
c
si429  L 0.2960 0.3085 0.3166 0.4681 0.5886 0.6044 0.6125
sp429  0.287 0.297 0.830 0.478 0.045 0.081 0.053
c
si430  L 0.2960 0.3085 0.3166 0.4681 0.5886 0.6044 0.6125
sp430  0.287 0.297 0.830 0.478 0.045 0.081 0.053
c
si431  L 0.2960 0.3085 0.3166 0.4681 0.5886 0.6044 0.6125
sp431     0.287 0.297 0.830 0.478 0.045 0.081 0.053
c
si432  L 0.2960 0.3085 0.3166 0.4681 0.5886 0.6044 0.6125
sp432     0.287 0.297 0.830 0.478 0.045 0.081 0.053
c
si433  L 0.2960 0.3085 0.3166 0.4681 0.5886 0.6044 0.6125
sp433     0.287 0.297 0.830 0.478 0.045 0.081 0.053
c
si434  L 0.2960 0.3085 0.3166 0.4681 0.5886 0.6044 0.6125
sp434     0.287 0.297 0.830 0.478 0.045 0.081 0.053
c
si435  L 0.2960 0.3085 0.3166 0.4681 0.5886 0.6044 0.6125
sp435     0.287 0.297 0.830 0.478 0.045 0.081 0.053
c
si436  L 0.2960 0.3085 0.3166 0.4681 0.5886 0.6044 0.6125
sp436     0.287 0.297 0.830 0.478 0.045 0.081 0.053
c
si437  L 0.2960 0.3085 0.3166 0.4681 0.5886 0.6044 0.6125
sp437     0.287 0.297 0.830 0.478 0.045 0.081 0.053
c
si438  L 0.2960 0.3085 0.3166 0.4681 0.5886 0.6044 0.6125
sp438     0.287 0.297 0.830 0.478 0.045 0.081 0.053
c
si439  L 0.2960 0.3085 0.3166 0.4681 0.5886 0.6044 0.6125
sp439     0.287 0.297 0.830 0.478 0.045 0.081 0.053
c
si440  L 0.2960 0.3085 0.3166 0.4681 0.5886 0.6044 0.6125
sp440     0.287 0.297 0.830 0.478 0.045 0.081 0.053
c
si441  L 0.2960 0.3085 0.3166 0.4681 0.5886 0.6044 0.6125
sp441     0.287 0.297 0.830 0.478 0.045 0.081 0.053
c
si442  L 0.2960 0.3085 0.3166 0.4681 0.5886 0.6044 0.6125
sp442     0.287 0.297 0.830 0.478 0.045 0.081 0.053
c
si443  L 0.2960 0.3085 0.3166 0.4681 0.5886 0.6044 0.6125
sp443     0.287 0.297 0.830 0.478 0.045 0.081 0.053
c
si444  L 0.2960 0.3085 0.3166 0.4681 0.5886 0.6044 0.6125
sp444     0.287 0.297 0.830 0.478 0.045 0.081 0.053
c
si445  L 0.2960 0.3085 0.3166 0.4681 0.5886 0.6044 0.6125
sp445     0.287 0.297 0.830 0.478 0.045 0.081 0.053
c
si446  L 0.2960 0.3085 0.3166 0.4681 0.5886 0.6044 0.6125
sp446     0.287 0.297 0.830 0.478 0.045 0.081 0.053
c
si447  L 0.2960 0.3085 0.3166 0.4681 0.5886 0.6044 0.6125
sp447     0.287 0.297 0.830 0.478 0.045 0.081 0.053
c
```

```
si448  L 0.2960 0.3085 0.3166 0.4681 0.5886 0.6044 0.6125
sp448     0.287 0.297 0.830 0.478 0.045 0.081 0.053
c
si449  L 0.2960 0.3085 0.3166 0.4681 0.5886 0.6044 0.6125
sp449     0.287 0.297 0.830 0.478 0.045 0.081 0.053
c
si450  L 0.2960 0.3085 0.3166 0.4681 0.5886 0.6044 0.6125
sp450     0.287 0.297 0.830 0.478 0.045 0.081 0.053
c
si451  L 0.2960 0.3085 0.3166 0.4681 0.5886 0.6044 0.6125
sp451     0.287 0.297 0.830 0.478 0.045 0.081 0.053
c
si452  L 0.2960 0.3085 0.3166 0.4681 0.5886 0.6044 0.6125
sp452     0.287 0.297 0.830 0.478 0.045 0.081 0.053
c
si453  L 0.2960 0.3085 0.3166 0.4681 0.5886 0.6044 0.6125
sp453     0.287 0.297 0.830 0.478 0.045 0.081 0.053
c
si454  L 0.2960 0.3085 0.3166 0.4681 0.5886 0.6044 0.6125
sp454     0.287 0.297 0.830 0.478 0.045 0.081 0.053
c
si455  L 0.2960 0.3085 0.3166 0.4681 0.5886 0.6044 0.6125
sp455     0.287 0.297 0.830 0.478 0.045 0.081 0.053
c
si456  L 0.2960 0.3085 0.3166 0.4681 0.5886 0.6044 0.6125
sp456     0.287 0.297 0.830 0.478 0.045 0.081 0.053
c
si457  L 0.2960 0.3085 0.3166 0.4681 0.5886 0.6044 0.6125
sp457     0.287 0.297 0.830 0.478 0.045 0.081 0.053
c
si458  L 0.2960 0.3085 0.3166 0.4681 0.5886 0.6044 0.6125
sp458     0.287 0.297 0.830 0.478 0.045 0.081 0.053
c
si459  L 0.2960 0.3085 0.3166 0.4681 0.5886 0.6044 0.6125
sp459     0.287 0.297 0.830 0.478 0.045 0.081 0.053
c
si460  L 0.2960 0.3085 0.3166 0.4681 0.5886 0.6044 0.6125
sp460     0.287 0.297 0.830 0.478 0.045 0.081 0.053
c
si461  L 0.2960 0.3085 0.3166 0.4681 0.5886 0.6044 0.6125
sp461     0.287 0.297 0.830 0.478 0.045 0.081 0.053
c
si462  L 0.2960 0.3085 0.3166 0.4681 0.5886 0.6044 0.6125
sp462     0.287 0.297 0.830 0.478 0.045 0.081 0.053
c
si463  L 0.2960 0.3085 0.3166 0.4681 0.5886 0.6044 0.6125
sp463     0.287 0.297 0.830 0.478 0.045 0.081 0.053
c
si464  L 0.2960 0.3085 0.3166 0.4681 0.5886 0.6044 0.6125
sp464     0.287 0.297 0.830 0.478 0.045 0.081 0.053
c
si465  L 0.2960 0.3085 0.3166 0.4681 0.5886 0.6044 0.6125
sp465     0.287 0.297 0.830 0.478 0.045 0.081 0.053
c
si466  L 0.2960 0.3085 0.3166 0.4681 0.5886 0.6044 0.6125
sp466     0.287 0.297 0.830 0.478 0.045 0.081 0.053
c
si467  L 0.2960 0.3085 0.3166 0.4681 0.5886 0.6044 0.6125
sp467     0.287 0.297 0.830 0.478 0.045 0.081 0.053
c
si468  L 0.2960 0.3085 0.3166 0.4681 0.5886 0.6044 0.6125
sp468     0.287 0.297 0.830 0.478 0.045 0.081 0.053
c
si469  L 0.2960 0.3085 0.3166 0.4681 0.5886 0.6044 0.6125
sp469     0.287 0.297 0.830 0.478 0.045 0.081 0.053
c
f6:p 960 961 962 963 964 965 966
c
c
nps 20000000
```